An Immune-Inspired Resource Allocation Strategy for Many-objective Optimization

Lingjie Li, Qiuzhen Lin, *Member, IEEE*, Zhong Ming, Ka-Chun Wong,
Maoguo Gong, *Senior Member, IEEE*, and Carlos A. Coello Coello, *Fellow*, *IEEE*

***Abstract*—Recently, a number of resource allocation strategies have been proposed for evolutionary algorithms to efficiently tackle multiobjective optimization problems (MOPs). However, these methods mainly allocate computational resources based on the convergence improvement under the decomposition-based framework, which may become ineffective with the increased number of optimization objectives. To address this problem, this paper suggests an immune-inspired resource allocation strategy, which breaks through the decomposition-based framework and can better balance convergence and diversity for many-objective optimization. In our method, the diversity distances of solutions are defined by the Euclidean distances of their projected points on the unit hyperplane. Then, based on the diversity distances, resource allocation is realized by using an immune cloning operator to encourage exploring sparse regions of the search space. Moreover, to provide high-quality solutions in coordination with this immune cloning operator, a novel archive update mechanism is designed. When compared to most well-known resource allocation strategies, our method is advantageous for many-objective optimization. The experimental results also validate the superiority of our method over several state-of-the-art evolutionary algorithms for solving two sets of complicated MOPs having 5 to 15 objectives.**

***Index Terms*—Many-objective optimization, Evolutionary algorithm, Resource allocation, Immune cloning operator**

I. Introduction

Multiobjective optimization problems (MOPs) involve the optimization of multiple objectives simultaneously [1]-[4], which can be mathematically defined by

$$\begin{aligned} &\text{minimize} \quad F(\mathbf{x}) = (f_1(\mathbf{x}),..., f_m(\mathbf{x})), \\ &\text{subject to} \quad \mathrm{x} \in \Omega, \end{aligned} \tag{1}$$

where $\mathbf{x} = (x_1,\ldots,x_n)$ is a decision vector in search space Ω (n means the number of decision variables) and $F(\mathbf{x})$ defines m objective functions. When m is larger than three, (1) is called a many-objective optimization problem (MaOP). As one single solution generally cannot optimize all objectives, a set of trade-off optimal solutions called Pareto-optimal set (PS) can be obtained and its mapping to the objective space is called Pareto-optimal front (PF) [5]. In recent decades, multiobjective evolutionary algorithms (MOEAs) have become very popular and effective for solving MOPs. Most MOEAs can be divided into three main categories based on the adopted population update mechanisms, i.e., Pareto-based MOEAs [6]-[10], decomposition-based MOEAs [11]-[13], and indicator-based MOEAs [14]-[18], which have been validated to be effective for solving MOPs with two or three objectives.

However, for solving many-objective optimization problems (MaOPs), MOEAs will face the following challenges [19]-[20]: (1) the Pareto dominance relationship becomes inefficient as most solutions become nondominated, (2) diversity is difficult to maintain, (3) the evolutionary operators become inefficient, and (4) the computational cost is extremely high. In order to address the above challenges, a number of studies have been conducted to enhance MOEAs for solving MaOPs, called many-objective evolutionary algorithms (MaOEAs). For Pareto-based MaOEAs, a hyperplane formed by the prominent solutions was designed in [21] and an effective fractional dominance relation was presented in [22], both of which can strengthen the convergence pressure toward the PF. For decomposition-based MaOEAs, reference vectors were adjusted adaptively in [23] and extracted from the population in [24] to dynamically track the PF shapes, and two new aggregation functions with distinct characteristics were designed in [25] to enhance the overall optimization performance. For indicator-based MaOEAs, the inverted generalized distance (IGD) indicator was used in [26] to select solutions with better convergence and diversity, and a more efficient indicator (ISDE+) was designed in [27] by summarizing the objective values and the shift-based density estimation, which can better solve various kinds of MaOPs. Moreover, a new voting-mechanism based ensemble framework called VMEF was presented in [28], which combines a number of different solution-sorting methods to effectively tackle MaOPs.

To the best of our knowledge, there are few studies to design resource allocation strategies (RASs) for MaOPs and most of the well-known RASs have been proposed for MOPs, which assign computational resources to individuals [29]-[34], evolutionary operators [35]-[36], weight vectors [37] or search subspaces [38]-[40]. Note that a brief review of existing RASs has been provided in **Section II-A**. Unfortunately, most existing RASs are not so effective for solving MaOPs, as they mainly allocate computational resources based on conver-

Manuscript received xx. xx. 2022; revised xx. xx. 2022; accepted xx. xx. 2022. This work was supported by the National Natural Science Foundation of China (NSFC) under Grants 61876110 and 61836005, Shenzhen Science and Technology Program Under Grants JCYJ20220531101411027 and JCYJ20190808164211203. Carlos A. Coello Coello gratefully acknowledges support from CONACyT grant no. 2016-01-1920 (Investigacion en Fronteras de la Ciencia 2016). (Corresponding authors: *Qiuzhen Lin* and *Zhong Ming*).

L.J. Li, Q.Z. Lin and Z. Ming are with the College of Computer Science and Software Engineering, Shenzhen University, Shenzhen 518060, China (e-mail of Lin: qiuzhlin@szu.edu.cn; Ming: mingz@szu.edu.cn).

Ka-Chun Wong is with the Department of Computer Science, City University of Hong Kong, Hong Kong, China.

M.G. Gong is with Key Laboratory of Intelligent Perception and Image Understanding of Ministry of Education, International Research Center for Intelligent Perception and Computation, Xidian University, Xi'an, Shanxi Province 710071, China.

C.A. Coello Coello is with the Department of Computer Science, CINVESTAV-IPN (Evolutionary Computation Group), México, D.F. 07300, MÉXICO. He is also with School of Engineering and Sciences, Tecnologico de Monterrey, Monterrey, N.L., Mexico.

gence improvement under the decomposition-based framework, which is difficult to maintain a final population with good diversity in high-dimensional objective spaces [41]-[42].

To fill this research gap, this paper proposes an immune-inspired resource allocation strategy (IRAS) for solving MaOPs, which aims to improve the effectiveness and robustness of RAS in high-dimensional objective spaces. Different from the existing traditional RASs, our proposed IRAS arranges the computation resources through an immune cloning operator rather than the aggregation metrics that are qualified under the decomposition-based framework. Specifically, IRAS considers the diversity distances of solutions to assign computational resources, which are defined as the Euclidean distances of their projected points on the unit hyperplane to estimate the diversity status. In this way, solutions with better diversity are cloned to be assigned computational resources, which are then mutated by evolutionary operators to generate offspring solutions for exploring sparse areas of the search space. Then, in order to reserve promising solutions from the parents and offspring, an efficient archive update mechanism (AUM) is designed to achieve a good trade-off between the diversity and convergence of the population. In summary, the proposed algorithm (called MaOEA/IRAS) iteratively runs IRAS, evolutionary operators, and AUM to solve MaOPs effectively. The main contributions of this paper are listed as follows:

1) To improve the performance of RAS in solving MaOPs, an immune-inspired resource allocation strategy (IRAS) is designed in this paper. Different from the existing RASs that use the aggregation metrics under the decomposition-based framework, our method adopts the immune cloning operator to achieve a reasonable assignment of computational resources. As experimentally validate in **Section IV**, our proposed IRAS is more effective than the existing RASs for solving MaOPs.

2) To reserve promising solutions for cloning, an archive update mechanism based on region division is designed to coordinate with the above IRAS, which can speed up convergence and maintain diversity by using two selection rounds.

In this study, two benchmark suites, i.e., WFG41-WFG48 [43] and MaF1-MaF13 [44] with a variety of PF shapes, are used to verify our performance. The experiments show that the proposed IRAS is superior over the existing RASs and the proposed MaOEA/IRAS is advantageous than several recently proposed MaOEAs in solving most of benchmark problems.

The remainder of this paper is organized as follows. **Section II** provides a short review of the existing RASs and clarifies our motivations. The details of MaOEA/IRAS are given in **Section III**, and the experimental results are provided in **Section IV**. Finally, our conclusions and future work are given in **Section V**.

II. Related Background and Motivations

A. A Short Review of Resource Allocation Strategies

As mentioned above, most of the existing RASs are designed for solving MOPs [29]-[40]. Here, a short review of RASs is provided next by classifying them into two main categories.

The first category of RASs assigns computational resources to individuals under the framework of MOEA/D [45], so that different individuals can obtain different resources to optimize their corresponding subproblems. In the original MOEA/D [45], all the subproblems are treated equally and are allocated the same quantities of computational resources. However, this method shows inefficiency when some decomposed subproblems are more difficult to be tackled than others [29]. To alleviate this issue, Zhang *et al*. proposed a dynamic resource allocation (DRA) strategy for MOEA/D [29]. In this method, the relative improvements on the aggregation function are considered for allocating computational resources and the subproblems having more improvements will receive more resources, as they have high potential to be further optimized. Then, Zhou *et al.* [30] extended DRA and presented a generalized resource allocation (GRA) strategy for MOEA/D. This approach builds the probability of improvement vector (PoI) for all subproblems, which is used to allocate computational resources by comparing PoI with random values in [0, 1]. Lin *et al.* [31] suggested a diversity-enhanced RAS to consider the relative improvements both in aggregation function values and the solution density around each subproblem using a weighted sum method. This approach has some advantages for solving MOPs with complicated PFs. Wang *et al.* [32] suggested a modified variant of DRA, which is more effective for solving MOPs with difficult-to-approximate PF boundaries. This study also verifies the importance of rational allocation of computational resources among different PF portions. Kang *et al.* [33] presented a collaborative resource allocation strategy for MOEA/D-M2M [46], termed MOEA/D-CRA. This approach dynamically assigns computational resources to subproblems according to their contributions and an external archive is employed to reserve the collaborative information during the search process. Wang *et al.* [34] proposed a new RAS for MOEA/D, called MOEA/D-RARS. This approach maintains a probability vector based on the relationship of subproblems to allocate computational resources.

The second category of RASs allocates computational resources to evolutionary operators [35]-[36], weight vectors [37], [45], and search subspaces [38]-[40], rather than individuals. For example, Li *et al.* [35] presented a bandit-based adaptive operator selection method for MOEA/D. In this approach, the evolutionary operators with high improvement rates will have more probabilities to be selected to optimize the subproblems, i.e., the evolutionary operators with better performance in the optimization process will receive more computational resources. Wang *et al.* [36] proposed an effective ensemble framework (called EF_PD) with competition and cooperation mechanisms. The evolutionary operators run a competition mechanism to receive more computational resources by using a decomposition-based credit assignment strategy, while the selection operator uses a cooperation mechanism to maintain superior solutions. Qi *et al.* [37] suggested an adaptive adjustment strategy for weight vectors in MOEA/D. In this approach, weight vectors are adaptively adjusted according to the distribution of the population, which

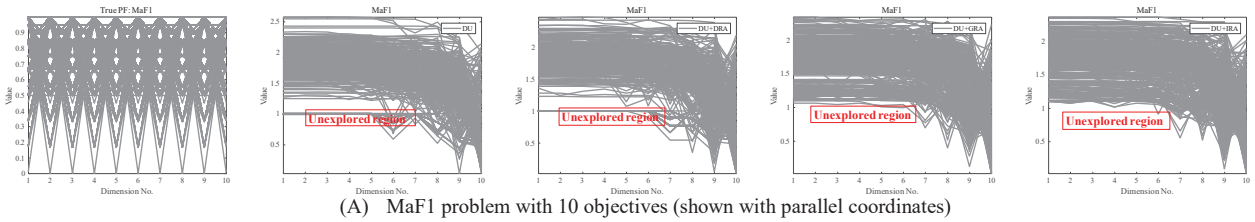

(A) MaF1 problem with 10 objectives (shown with parallel coordinates)

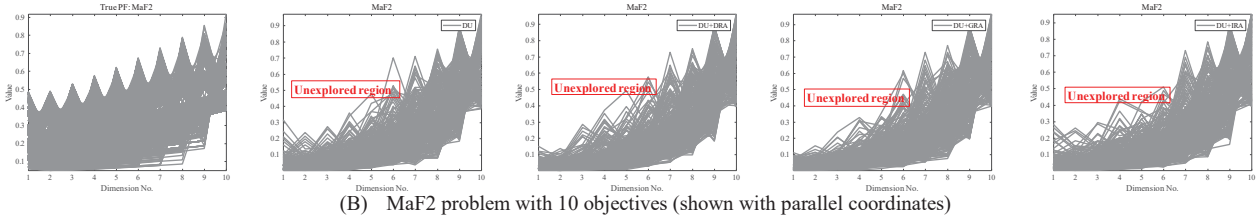

(B) MaF2 problem with 10 objectives (shown with parallel coordinates)

Fig. 1: Final solution sets obtained by MOEA/D-DU and its three new variants combined with different RASs and the true PF for MaF1 and MaF2 problems

are allocated more in the actually sparse regions. Thus, more computational resources are assigned to explore these regions. Wang *et al.* [38] designed an adaptive region adjustment strategy (ARA) to assign more computational resources to the subregions with better performance. They [39] also proposed a dynamic allocation for preferences based on a differential space. With the decomposition method, a reference vector is used to divide an objective into several subspaces and then the numbers of preferences (i.e., computation resources) are allocated based on the selection pressure within the subspaces. Liu *et al.* [47] suggested to adaptively allocate search efforts in different sub-regions according to the importance of different objectives. In this method, more computational resources (i.e., search efforts) are devoted to exploring potential promising sub-regions, which helps to address some challenges when tackling MaOPs with various PFs. Furthermore, Chen *et al.* [40] also developed an objective space partition-based method to adaptively allocate different resources for various subspaces based on their corresponding contributions, which are measured by the forward pushed distance.

B. Motivations

Here, the motivations of this paper are clarified from both theoretical and empirical analyses, as follows:

Theoretical analysis: As reviewed in **Section II-A**, most of the existing RASs [29]-[31], [35]-[36] are designed under the decomposition-based framework, which can properly solve MOPs with two or three objectives. However, when solving MaOPs, they are difficult to specify a suitable set of weight vectors to properly match various irregular PF shapes in high-dimensional objective spaces. As pointed out in [48]-[49], the performance of decomposition-based MOEAs strongly depends on the fitting degree to the shapes of weight vectors and PFs. Thus, a number of research studies have been conducted in [23]-[24], [45], [50]-[51] to enhance the performance of decomposition-based MOEAs for solving MaOPs, which try to automatically adjust the weight vectors and then guide the evolutionary search toward different parts of PF. However, as pointed out in [52]-[54], these frequent changes of weight vectors may deteriorate the convergence speed of solutions. Thus, this paper would like to design a new RAS that breaks through the decomposition-based framework and can significantly improve the performance of RAS for solving MaOPs.

TABLE I
SUMMARY OF SIGNIFICANCE TEST BETWEEN DU AND THREE VARIANTS COMBINED WITH THREE RASS (DRA, GRA AND IRA) BASED ON HV

Comparisons based on		Test problems	DU+DRA vs. DU			DU+GRA vs. DU			DU+IRA vs. DU		
			–	~	+	–	~	+	–	~	+
No. (m)	m=5	WFG4X	0	8	0	0	4	4	0	4	4
		MaF	3	1	3	1	1	5	2	2	3
	m=10	WFG4X	3	5	0	0	1	7	0	2	6
		MaF	3	2	2	3	1	3	4	1	2
	All		9	16	5	4	7	19	7	9	14

Empirical analysis: To empirically study the performance of the existing RASs for solving MaOPs, three widely used RASs (DRA [29], GRA [30] and IRA [31]) are first embedded into MOEA/D-DU [55], and the three variants are called DU+DRA, DU+GRA and DU+IRA, respectively. All the parameters in these compared algorithms are set as suggested in their original references. Due to page limitations, the detailed HV [56] results of these compared variants for solving the test problems used in this paper (i.e., WFG41-WFG48 [43] and MaF1-MaF7 [44] with 5 and 10 objectives) are provided in Tables A. I-A. II of the supplementary file. Moreover, the summary of the significance test for HV values in each comparison is listed in Table I, where the numbers under the columns "-", "~" and "+" indicate the comparison times that the results of MOEA/D-DU combined with three different RASs are better than, statistically similar with and worse than that of the original MOEA/D-DU, respectively. The last row of Table I summarizes the results. When compared to DU+DRA, DU+GRA and DU+IRA in a total of 30 cases, MOEA/D-DU performs better in 5, 19 and 14 cases, worse in 9, 4 and 7 cases, and similarly in 16, 7 and 9 cases, respectively. In addition, to visually show the performance of these RASs, the final solutions of these three variants for solving MaF1 and MaF2 with 10 objectives are plotted in Fig. 1-(A) and Fig. 1-(B), respectively. As observed from these figures, MOEA/D-DU shows poor diversity when solving MaF1 and MaF2 with 10 objectives. However, the three variants of MOEA/D-DU combined with DRA, GRA and IRA also encounter the same issue of maintaining diversity. Thus, the existing RASs fail to improve the performance of MOEA/D-DU on the 10-objective MaF1

and MaF2 problems, mainly because they use the relative improvements of aggregation function values as the metric for resource allocation under the decomposition-based framework, so that few computational resources are allocated to reproduce solutions for exploring these regions. Moreover, these empirical results also demonstrate that the existing RASs are not so efficient for solving MaOPs.

Based on the above theoretical and empirical analyses, the existing RASs under the decomposition-based framework still face challenges and are experimentally validated to be inefficient for solving MaOPs. Thus, this paper suggests a new immune-inspired resource allocation strategy (IRAS), which applies the immune cloning operator rather than the decomposition-based methods to achieve a reasonable assignment of computational resources when solving MaOPs. The details of our proposed method are introduced in next section.

III. The Proposed Algorithm

In this section, the details of the proposed IRAS and the proposed algorithm (MaOEA/IRAS) are introduced. First, the main flowchart of the proposed MaOEA/IRAS is plotted in Fig. 2 for better understanding. In the following subsections, the framework of MaOEA/IRAS is introduced in **Section III-A**. Then, the details of IRAS are given in **Section III-B**, and the details of the proposed archive update mechanism are introduced in **Section III-C**.

A. The Framework of MaOEA/IRAS

The pseudocode of MaOEA/IRAS is given in **Algorithm 1** with the inputs: N (the population size) and *MaxGen* (the maximum number of generations). As shown in line 1, the population P is initialized by randomly generating N solutions in the decision space. Then, some parameters in MaOEA/IRAS are initialized in line 2 by setting $Gen = 0$ (the current number of generations), $c_i = 0$ (the cloning number for the i^{th} solution). $Z_i^* = (z_1^*, z_2^*, ..., z_m^*)$ and $Z_i^{nadir} = (Z_1^{nadir}, Z_2^{nadir}, ..., Z_m^{nadir})$ are the ideal point and nadir point of the population, respectively, where m is the number of objectives. After that, the main loop of MaOEA/IRAS starts. If the termination condition is not satisfied in line 3, the proposed IRAS is first run in line 4 to generate the cloned population C. The details of IRAS are given in **Algorithm 2**, which will be introduced in **Section III-B**. In lines 5-6, the cloned population C will undergo two popular evolutionary operators, i.e., simulated binary crossover (SBX) [57] and polynomial-based mutation (PM) [58]. When selecting two parents for the SBX operator, the first one is randomly selected from the top λ of solutions with the minimized summation of objective values (we set λ =20% in this paper and the parameter tuning of λ is provided in Table A. III of the supplementary file), while the second one is randomly selected from the whole population C. In line 7, all the offspring in C' are combined with the parent population P to form a union population U. Then, the archive update method is used for U to select N solutions with promising performance, which can coordinate with the proposed IRAS. All the selected solutions are updated as the new population P for next iteration.

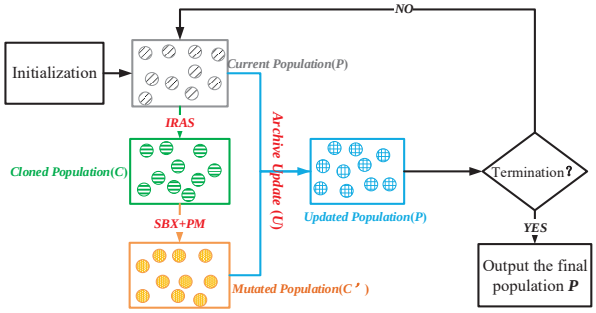

Fig. 2 The flowchart of the proposed MaOEA/IRAS.

Algorithm 1: The complete framework of MaOEA/IRAS

Input: N, *MaxGen*;
Output: the population P;
1: initialize the population P;
2 initialize Gen, c_i, Z_i^* and Z_i^{nadir};
3: **while** Gen<*MaxGen*
4: C=**IRAS** (P);//**Algorithm 2**
5: C'=*Crossover* (C);
6: C'=*Mutation* (C');
7: U= *Union* (P, C');
8: P= **Archive Update** (U)//**Algorithm 3**
10: update Z_i^* and Z_i^{nadir};
11: Gen=Gen+1;
12: **end while**

The details of the proposed archive update method are introduced in **Section III-C**. Finally, all the solutions in the final population P are reported as the final approximation set when Gen reaches *MaxGen*.

B. An Immune-Inspired Resource Allocation Strategy

Unlike MOEAs, many multiobjective immune algorithms (MOIAs) [59]-[60] have been proposed with unique cloning operators, which are inspired from the body immune response principles of natural immune system (NIS). Regarding the clonal selection principle in NIS, only antigen-aware cells can be amplified. Similar to the NIS, the principle of clonal selection in MOIAs is that only these individuals with good performance will be selected as parents for cloning. In this way, more cloned offspring with better performance can be generated to improve the overall performance of the population. In order to have an easy understanding of the immune cloning operator, due to page limitations, its schematic diagram is plotted in Fig. A.1 of the supplementary file. More details of MOIAs please refer to our previous published survey [61]. Moreover, extensive empirical results in [62]-[64] demonstrate that MOIAs can provide a high convergence speed and maintain the population's diversity. Inspired by this, this paper attempts to combine the concept of RAS with the immune cloning operator. In our design, the proposed IRAS is realized by using an immune cloning operator rather than the fitness values that are qualified by the decomposition-based methods. In this way, solutions with many clones are preferentially assigned with more computational resources. Here, the cloning operator is constructed as follows:

$$C = \bigcup_{i=1}^{N} \{c_i \otimes \mathbf{x}_i\}, \mathbf{x}_i \in P, \quad (2)$$

Algorithm 2: C= **IRAS** (P)
Input: the current population P;
Output: the cloned population C;
1: **for** i=1 to $|P|$
2: calculate the diversity distance dis_i by using (4);
3: **end for**
4: **for** i=1 to $|P|$
5: **while** $|C|<N$
6: sort all the solutions in ascending order based on dis_i ;
7: build the neighbor set for each solution;
8: compute c_i by using (3);
9: clone each solution to generate offspring by using (2);
10: add all the offspring to C;
11: **end while**
12: **if** $|C|>N$ **then**
13: recalculate the dis_i for each solution in C;
14: delete the solution with the smallest dis_i from C;
15: **end if**
16: **end for**

where $\otimes$ indicates the cloning operator. c_i is the number of clones for solution $\mathbf{x}_i$, as calculated by

$$c_i = \left\lceil N \times \frac{min\left\{dst_i^1\left\langle \mathbf{x}_i, \mathbf{x}_1\right\rangle, dst_i^2\left\langle \mathbf{x}_i, \mathbf{x}_2\right\rangle, ..., dst_i^T\left\langle \mathbf{x}_i, \mathbf{x}_T\right\rangle\right\}}{sum\left\{dst_i^1\left\langle \mathbf{x}_i, \mathbf{x}_1\right\rangle, dst_i^2\left\langle \mathbf{x}_i, \mathbf{x}_2\right\rangle, ..., dst_i^T\left\langle \mathbf{x}_i, \mathbf{x}_T\right\rangle\right\}} \right\rceil \tag{3}$$

where $i \in [1, N]$, T is the size of the neighbor set for solution $\mathbf{x}_i$ (T is set to $0.1\times N$ as in [65]-[66] and more discussions on different settings of T are given in Section 2 of the supplementary file), and $\left\{dst_i^1\left\langle \mathbf{x}_i, \mathbf{x}_1\right\rangle, dst_i^2\left\langle \mathbf{x}_i, \mathbf{x}_2\right\rangle, ..., dst_i^T\left\langle \mathbf{x}_i, \mathbf{x}_T\right\rangle\right\}$ denotes the T closest diversity distances [67] between $\mathbf{x}_i$ and its neighbors, as computed by

$$dst_i^j\left\langle \mathbf{x}_i, \mathbf{x}_j\right\rangle = \left\| \lambda(\mathbf{x}_i) - \lambda(\mathbf{x}_j) \right\|_2 \quad i \in [1, N], j \in [1, T] \wedge i \neq j \tag{4}$$

$$\text{with } \lambda(\mathbf{x}_i) = \frac{1}{\sum_{h=1}^{m} f_h^{'}(\mathbf{x}_i)} \times F^{'}(\mathbf{x}_i) , \tag{5}$$

where $\| \lambda(\mathbf{x}_i) - \lambda(\mathbf{x}_j) \|_2$ denotes the 2-norm of a vector. $F^{'}(\mathbf{x}_i) = \left(f_1^{'}(\mathbf{x}_i), f_2^{'}(\mathbf{x}_i), ..., f_m^{'}(\mathbf{x}_i)\right)^T$ is the normalized objective vector, m is the number of objectives, and $f_h^{'}(\mathbf{x}_i)$ indicates the h^{th} normalized objective vector for solution $\mathbf{x}_i$, as defined by:

$$f_h^{'}(\mathbf{x}) = \frac{f_h(\mathbf{x}) - Z_h^*}{Z_h^{nadir} - Z_h^*}, \ h \in [1, m] \ , \tag{6}$$

where Z_h^* and Z_h^{nadir} are respectively the ideal point and the nadir point of the population, and m indicates the number of objectives. Hence, the diversity distance value for each solution $\mathbf{x}_i$ in population P can be denoted as dis_i (i.e., $dis_i \left|_{i=1}^{N} = min\left\{dst_i^1\left\langle \mathbf{x}_i, \mathbf{x}_1\right\rangle, dst_i^2\left\langle \mathbf{x}_i, \mathbf{x}_2\right\rangle, ..., dst_i^T\left\langle \mathbf{x}_i, \mathbf{x}_T\right\rangle\right\}\right.$). Due to page limitations, the reasons for using the diversity distance instead of the traditional angle value are discussed in Section 3 of the supplementary file.

The pseudocode of the proposed IRAS is given in **Algorithm 2** with the input: P (the current population).The diversity distance between each solution and all others is calculated by using (4) in lines 1-3. Then, the T-closest solutions are selected based on the corresponding dis_i values to build the neighbor set in line 7. Next, the number of clones for each solution is calculated in line 8. According to (3), more clones are allocated for the solutions with large dis_i values. Then, the cloning operator is run to generate offspring based on (2) in line 9. Finally, an archive truncation process is performed in lines 12-15 to ensure that the cloned population size is equal to N.

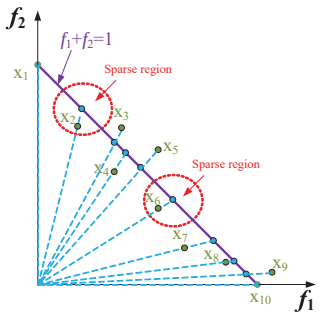

Fig. 3 A simple example of the diversity distance for each solution

A simple example is provided in Fig. 3 to explain the diversity distance between each solution and others. As shown in Fig. 3, solutions $\mathbf{x}_2$ and $\mathbf{x}_6$ have larger diversity distance values than other solutions in the population (e.g., $\mathbf{x}_3$, $\mathbf{x}_4$, $\mathbf{x}_8$ and $\mathbf{x}_9$). In other words, solutions $\mathbf{x}_2$ and $\mathbf{x}_6$ are located in sparse regions. Hence, according to the principle of the proposed IRAS, solutions $\mathbf{x}_2$ and $\mathbf{x}_6$ are allocated more computational resources than other solutions and more offspring are cloned to explore the sparse regions in which they are located. That is, more computational resources can be allocated to generate more promising solutions in these sparse regions, which have large survival potential in the subsequent archive update step, thus improving the diversity of population when solving MaOPs in high-dimensional objective spaces.

C. An Efficient Archive Update Mechanism

To provide high-quality solutions for the cloning operator, an efficient archive update mechanism, denoted as AUM, is proposed in MOEA/IRAS. **Algorithm 3** presents the pseudocode of AUM. As shown in lines 1-2, the process of subregion division is run, where the objective space Ω is divided into K uniform subregions based on the diversity distance dis_i, which aims to guarantee the distribution of the population. In this paper, we set K=$\lceil N \times (m-1)/m \rceil$, where m and N are the number of objectives and the population size, respectively. Note that the parameter tuning of K is provided in Table A. IV of the supplementary file. Particularly, K solutions in the union population U with lager diversity distances and uniform distribution are used to construct K uniform subregions. Then, an association procedure is performed for the remaining solutions in U, where each solution is associated with the closest unique subregion according to the diversity distance in (4).

After the division procedure, two selection rounds are run. In the first round of selection, one solution with the smallest average diversity distance value in the k^{th} subregion is selected, which is formulated as follows:

$$avgdis_r^k = \frac{\sum_{l=1}^{|R_k|} dst_r^l\left\langle \mathbf{x}_r, \mathbf{x}_l\right\rangle}{|R_k|} , \tag{7}$$

where k is the index of the k^{th} subregion (i.e., $k \in [1, K]$), r and l are the indexes of solutions in subregion R_k ($r, l \in [1, |R_k|]$

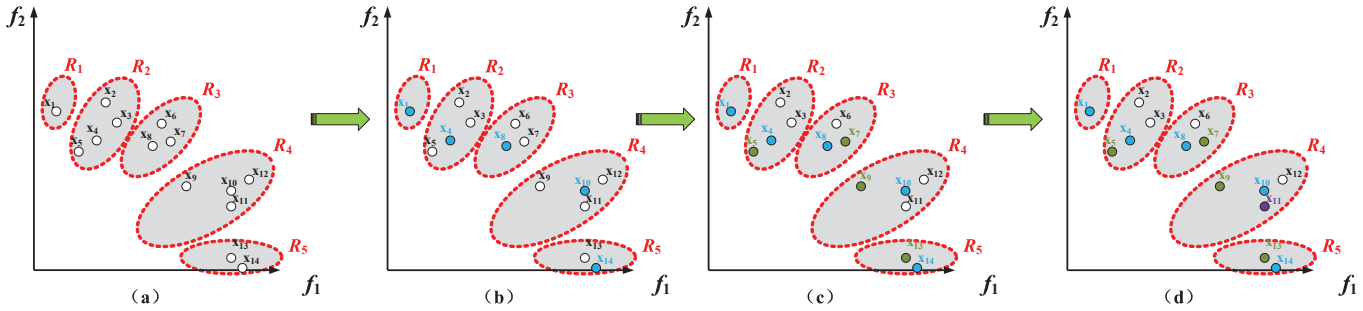

Fig. 4: The process of the proposed archive update mechanism (AUM) with (a) region division process; (b) the selected solutions with the best representative distribution in each subregion; (c)-(d) the selected solutions with the best convergence in each subregion.

Algorithm 3: P= **Archive Update** (U)

Input: the union population U;
Output: the new population P;
1: //*The process of subregion division*
2: divide the objective space into K subregions based on the diversity distance dis_i ;
3: **for** k= 1 to K
4: **for** r= 1 to $|R_k|$
5: calculate the $avgdis_r^k$ using (7);
6: **end for**
7: **end for**
8: //*Frist round of selection in archive update*
9: **for** k= 1 to K
10: select the solution with the smallest $avgdis_r^k$ in R_k;
11: add the selected solution to P and remove it from R_k;
12: **end for**
13: //*Second round of selection in archive update*
14: *Remains*=*N*-*K*;
15: **if** *Remains* > *K*
16: **for** k= 1 to K
17: select the solution with the smallest sum value of objectives in R_k;
18: add the selected solution to P and remove it from R_k;
19: *Remains*=*Remains*-1;
20: **end for**
21: **else**
22: select the remaining solutions from |*Remains*| random subregions.
23: **end if**

and $r \neq l$). $avgdis_r^k$ is the average diversity distance value for the solution $\mathbf{x}_r$ in the k^{th} subregion, $dst_r^l\langle \mathbf{x}_r, \mathbf{x}_l \rangle$ indicates the diversity distance value between the solution $\mathbf{x}_r$ and other solutions in the k^{th} subregion calculated by using (4). In this way, one solution with the best representative distribution (i.e., with the smallest diversity distance value) in each subregion is selected and a total of K solutions are obtained in the first selection round, which aims to guarantee the population's diversity. After that, the remaining $N-K$ solutions with best convergence are selected in the second round, which is based on the sum of objective function values. Hence, the diversity and convergence of the population can be guaranteed simultaneously through the use of our archive update strategy.

As shown in lines 8-12 of **Algorithm 3**, K solutions with the smallest average diversity distance value in each corresponding subregion are selected in the first selection round. For the chive update process will continue until the new population P is full. Specially, when the number of solutions that are needed to be selected is larger than the number of subregions (i.e., *Remains*>*K*), the solutions are sequentially selected from each subregion according to their corresponding sum of the objective function values in lines 14-20. Otherwise, the remaining solutions with the smallest sum of objective function values are selected from |*Remains*| random subregions in line 22. Thus, MaOEA/IRAS adopts a diversity first and convergence second principle [68]-[69] to perform the environmental selection, which gives priority to preserve the individual with the best representative distribution in each subregion.

To facilitate the understanding of the proposed archive update strategy, a simple example is given in Fig. 4 that shows the archive update process in a normalized bi-objective space. First, the objective space is divided uniformly into five subregions (e.g., R_1, R_2, R_3, R_4, and R_5) in Fig. 4(a), which is based on the diversity distance of each solution to others. After that, the first selection round is performed in Fig. 4(b), where the five solutions (marked as the blue circles: $\mathbf{x}_1$, $\mathbf{x}_4$, $\mathbf{x}_8$, $\mathbf{x}_{10}$, and $\mathbf{x}_{14}$) with the smallest average diversity distances $avgdis_r^k$ calculated by (7) are selected and added to construct the new population P from the union population U to ensure a reasonable population distribution. It should be noted that the diversity distance for the boundary solutions is set to half of the minimum diversity distance. Then, the second selection round in the archive update is performed in Figs. 4(c)-(d). In Fig. 4(c), $\mathbf{x}_5$, $\mathbf{x}_7$, $\mathbf{x}_9$ and $\mathbf{x}_{13}$ are selected in turn (marked by the green circles) because their aggregated objective values are smallest in the corresponding subregions. When |*Remains*|>*K*, the last few solutions will be selected from |*Remains*| random subregions. As shown in Fig. 4(d), the last solution is selected from subregion R_4 (i.e., $\mathbf{x}_{11}$ marked with the purple circle) when P is not full. Finally, $\mathbf{x}_1$, $\mathbf{x}_4$, $\mathbf{x}_8$, $\mathbf{x}_{10}$, $\mathbf{x}_{14}$ with the best representative distribution and $\mathbf{x}_5$, $\mathbf{x}_7$, $\mathbf{x}_9$, $\mathbf{x}_{13}$ with the best convergence in each subregion are added into the archive after the process of archive update.

IV. Experimental Studies

A. Benchmark Problems and Quality Indicators

1) Benchmark Problems:

In our experimental studies, fifteen benchmark problems were used to assess the performance of the proposed algorithm MaOEA/IRAS, including WFG41-WFG48 [43] and MaF1-MaF13 [44] with a variety of PF shapes. These adopted test problems have different PFs, which can be used to effectively assess the performance of different MOEAs. WFG42, WFG44 and MaF3 have convex PFs, while WFG41, WFG43 and MaF5 have concave PFs. Particularly, WFG44 has a strong convex PF, and WFG43 has an extremely concave PF. Moreover, both MaF1 and MaF4 have inverted PFs, MaF6 shows a degenerated PF, WFG46 has a regular linear PF, MaF7 and MaF11 have disconnected PFs, MaF8 and MaF9

have linear and degenerate PFs, MaF12 and MaF13 have concave PFs. The PFs for the remaining problems (i.e., WFG45, WFG47 and WFG48, MaF10) are mixed and complicated. Thus, these adopted problems can be used to validate the robustness of MaOEAs for solving MaOPs with different PFs.

The number of objectives m ranges from 5 to 15 in our experimental comparison, where $m \in \{5,8,10,13,15\}$. In addition, as suggested in [44], the number of decision variables n in MaF1-MaF7 was set based on $n = m+k-1$, where k was set to 10 for MaF1-MaF6 and to 20 for MaF7, n was set to 2 for MaF8 and MaF9 and to 5 for MaF13. For MaF10-MaF12 and WFG41-WFG48, the decision variables consist of k position-related parameters and l distance-related parameters. As introduced in [43], k was set to $2\times(m-1)$, and l was set to 20.

2) Quality Indicator:

Regarding the quality indicator for the final solutions obtained by MOEAs, the hypervolume (HV) indicator [56] was used in our experimental studies to assess both convergence and spread. HV is the hypervolume of the space between the nondominated solutions and a reference point. A larger HV value indicates a good approximation to the true PF. Note that solutions dominated by the reference point are not included in the calculation of the HV, and the setting of the reference point is crucial for the calculation of the HV. In this study, to have a fair comparison, the reference point for computing the HV is set as suggested in [70], in which the objective values of the final solutions are all normalized first by using $1.1\times(Z_1^{nadir}, Z_2^{nadir}, ..., Z_m^{nadir})$, where Z_h^{nadir} indicates the h-th nadir point of the true PF ($h \in [1, m]$), and then the reference points are set to (1.0, 1.0, …, 1.0). Notably, to avoid the situation that the HV values obtained by the compared algorithms are very small and close to zero, the reference points are set as (2.0, 2.0, …, 2.0) for MaF1 with more than 10 objectives (i.e., $m \in \{10,13,15\}$). Moreover, a Monte Carlo simulation methods [71] with 10^7 sampling points is adopted to approximately calculate the HV values when the test problems have more than 8 objectives (i.e., $m \in \{8,10,13,15\}$).

B. Parameter Settings for the Compared Algorithms

In our experimental studies, to verify the effectiveness of the proposed IRAS in high-dimensional objective spaces, three well-known RASs, including DRA [29], GRA [30], and IRA [31], are compared with the proposed IRAS. Then, to further verify the advantages of the proposed MaOEA/IRAS, six competitive MaOEAs are also included for comparison, including RVEAiGNG [72], PeEA [73], MOEA/AD [74], MaOEA/IGD [21], MaPSO [75] and hpaEA [26]. Note that all the compared MaOEAs were independently run with 30 times for each test problem on a personal computer with an Intel (R) Core (TM) i7-6700 CPU, 3.40 GHz (processor), and 20 GB (RAM).

Regarding the evolutionary operators, SBX [57] and PM [58] were used for all the compared MaOEAs, except for MaPSO that adopted the PSO search strategy. p_c and p_m are the probabilities of crossover and mutation, respectively. η_c and η_m are the distribution indexes of SBX and PM, respectively. Other experimental parameters were configured with the same values as in the corresponding references. These values are summarized in Table A. V of the supplementary file.

The population sizes for different numbers of objectives are summarized in Table A. VI of the supplementary file. For test problems with 5, 8, 10, 13 and 15 objectives, the number of weight vectors were set to 210, 240, 275, 182 and 240, respectively, by using the two-layer generation method with the simplex-lattice design factor H, as suggested in [76]. All the algorithms are terminated when the preset maximum number of generations G_{max} is reached. The settings of G_{max} for different numbers of objectives are also listed in Table A. VI. For each algorithm, the maximum function evaluations (*MFE*) can be easily determined by $MFE = N\times G_{max}$.

C. Comparisons with Different RA strategies

To verify the superiority of IRAS over three conventional RASs (i.e., DRA [29], GRA [30] and IRA [31]), experimental comparisons were conducted. Please note that MaOEA/IRAS uses an efficient archive update mechanism (AUM), which is different from the archive update strategies in DRA, GRA and IRA. Hence, for a fair comparison of different RASs, the proposed AUM was also embedded into DRA, GRA and IRA, yielding three new variants called DRA+AUM, GRA+AUM and IRA+AUM, respectively. To unify the format, the proposed IRAS, which includes IRAS and AUM, was abbreviated as IRAS+AUM. Due to page limitations, the effectiveness of our proposed AUM has been validated based on the experimental results summarized in Table A. VII and Table A. VIII of the supplementary file. Note that the symbols in the tables "-", "~" and "+" indicate our proposed method is better than, statistically similar with and worse than the compared algorithm, respectively, based on the Wilcoxon rank sum test with a 0.05 significant level.

1) Comparison Results based on WFG41-WFG48

Table A. IX of the supplementary file provides a comparison of results in terms of the HV for WFG41-WFG48 with 5 to 15 objectives (m=5, 8, 10, 13, and 15). Some conclusions can be drawn from the HV results listed in Table A. IX. As summarized in the second-to-last row of the table, IRAS+AUM shows an obvious superiority over the other methods, because it obtains the best results in 39 out of 40 cases, and the competitors that use other RASs (DRA, GRA and IRA) obtain the best results in 0, 0 and 1 out of 40 cases. The main difference between the compared algorithms is the applied RASs. Hence, the obvious advantages of the proposed IRAS in solving WFG4X with many objectives are verified based on the HV results listed in Table A. IX. Furthermore, from the one-by-one comparisons in the last row of Table A. IX of the supplementary file, IRAS+AUM also performs better than DRA+AUM, GRA+AUM and IRA+AUM in 40, 40 and 39 out of 40 cases, respectively, and only shows a slight disadvantage when compared with IRA+AUM for WFG43 with 13 objectives. In particular, DRA, GRA and IRA assign computational resources according to the relative improvement of the aggregated function value, which showed difficulty to maintain diversity in solving MaOPs. Whereas, the proposed IRAS allocates computational resources by using the diversity distance to enhance diversity, which is beneficial for solving MaOPs. Thus, the superior performance of IRAS+AUM here

further validates the effectiveness of the proposed IRAS, which can improve the ability to maintain diversity in a high-dimensional objective space.

2) Comparison Results based on MaF1-MaF13

Table A. X of the supplementary file gives a comparison of results for all the considered algorithms in terms of HV on MaF1-MaF13 with 5 to 15 objectives (m=5, 8, 10, 13, and 15). As indicated in the second-to-last row of Table A. X of the supplementary file, IRAS+AUM shows superior performance when compared to other methods, as it yields the best results in 48 out of 65 cases, while DRA+AUM, GRA+AUM and IRA+AUM only have the best results in 6, 0 and 11 out of 65 cases, respectively. From the last row of Table A. X, IRAS+AUM performs better than DRA+AUM, GRA+AUM and IRA+AUM in 53, 53 and 48 out of 65 cases, respectively, while it is only outperformed in 8, 8 and 12 out of 65 cases. Therefore, it is reasonable to conclude that IRAS+AUM showed superior performance over its three competitors that use traditional RASs in solving most of the MaF1-MaF13 problems.

3) Further Discussion and Analysis of the Overall Performance of Compared RASs

Table II summarizes the significance test results based on the HV for each comparison. To ensure a statistically sound conclusion, the Wilcoxon rank sum test with a 0.05 significance level and the Wilcoxon signed-rank test from the platform KEEL [77] were used, where the results display statistically significant differences on the HV. Moreover, an asymptotic p-value obtained based on the Wilcoxon signed-rank test and the KEEL tool is shown in the column "p-value". It should be noted that a p-value close to zero indicates that there are significant differences among the compared algorithms based on the HV results.

Regarding the results summarized in Table II for various test problems ranging from 5 to 15 objectives, some conclusions can be drawn. When considering all the WFG4X test problems, the proposed IRAS+AUM shows an absolute superiority over the other algorithms. IRAS+AUM obtains all the best results for the WFG4X test problems with various objectives except for WFG43 with 13 objectives. Considering the PF shape of WFG4X, WFG43 has a strong concave PF while WFG44 has an extremely convex PF. Thus, the advantages of IRAS+AUM on WFG43 and WFG44 have validated the effectiveness of the proposed IRAS for solving such problems with extremely convex/concave PFs. WFG47 and WFG48 both have disconnected and concave PFs. The superiority of IRAS+AUM over other methods on WFG47 and WFG48 is mainly due to the running of the proposed IRAS that uses the diversity distance to assign computational resources, while other RASs use the relative improvement of the aggregated function values based on a set of uniform weight vectors, which has some drawbacks in solving problems with disconnected PFs [42], [46].

When considering all the MaF test problems, the proposed IRAS displays some advantages when compared to other traditional RASs (DRA, GRA and IRA). Considering MaF4 with an irregular PF, which was derived from DTLZ3 by inverting the PF shape, IRAS+AUM obtains all the best results for the MaF4 test problem on all the objectives adopted in this paper. Hence, the superiority of IRAS+AUM for MaF4 confirms the advantages of the proposed IRAS in solving some problems with irregular PFs. However, the decomposition-based RASs failed, because it is hard to specify a set of weight vectors that can highly fit to the PF with various irregular shapes. Remarkably, for MaF3 with a multimodal PF, IRA+AUM shows superior performance over the other methods in the cases of 10, 13, and 15 objectives. When dealing with MaF11 that has a scaled disconnected PF, our method is slightly inferior to other competitors.

TABLE II
SUMMARY OF SIGNIFICANCE TEST BETWEEN IRAS+AUM AND THREE RASS (DRA, GRA AND IRA) COMBINED WITH AUM ON HV

Comparisons based on		IRAS+AUM vs. DRA+AUM				IRAS+AUM vs. GRA+AUM				IRAS+AUM vs. IRA+AUM			
		–	~	+	p-value	–	~	+	p-value	–	~	+	p-value
Test Problems	WFG41	**5**	**0**	**0**	**0.0500**	**5**	**0**	**0**	**0.0071**	**5**	**0**	**0**	**0.0071**
	WFG42	**5**	**0**	**0**	**0.0048**	**5**	**0**	**0**	**0.0022**	**5**	**0**	**0**	**0.1416**
	WFG43	**5**	**0**	**0**	**0.1416**	**5**	**0**	**0**	**0.0071**	**4**	**0**	**1**	**0.0275**
	WFG44	**5**	**0**	**0**	**0.0071**	**5**	**0**	**0**	**0.0071**	**5**	**0**	**0**	**0.0500**
	WFG45	**5**	**0**	**0**	**0.0199**	**5**	**0**	**0**	**0.0048**	**5**	**0**	**0**	**0.0274**
	WFG46	**5**	**0**	**0**	**0.0500**	**5**	**0**	**0**	**0.0143**	**5**	**0**	**0**	**0.0033**
	WFG47	**5**	**0**	**0**	**0.0500**	**5**	**0**	**0**	**0.0014**	**5**	**0**	**0**	**0.0276**
	WFG48	**5**	**0**	**0**	**0.0015**	**5**	**0**	**0**	**0.0101**	**5**	**0**	**0**	**0.1113**
	MaF1	**5**	**0**	**0**	**0.0374**	**4**	**1**	**0**	**0.0373**	**5**	**0**	**0**	**0.0015**
	MaF2	**5**	**0**	**0**	**0.0022**	**5**	**0**	**0**	**0.0101**	**5**	**0**	**0**	**0.0864**
	MaF3	**4**	**1**	**0**	**0.1779**	**3**	**1**	**1**	**0.1779**	1	1	3	0.4624
	MaF4	**5**	**0**	**0**	**0.0500**	**5**	**0**	**0**	**0.0006**	**5**	**0**	**0**	**0.0500**
	MaF5	**5**	**0**	**0**	**0.0015**	**5**	**0**	**0**	**0.0033**	**5**	**0**	**0**	**0.2206**
	MaF6	**5**	**0**	**0**	**0.0143**	**5**	**0**	**0**	**0.0275**	**5**	**0**	**0**	**0.0071**
	MaF7	**4**	**0**	**1**	**0.0048**	**3**	**1**	**1**	**0.1113**	2	0	3	**0.3272**
	MaF8	**4**	**0**	**1**	**0.0864**	**4**	**0**	**1**	**0.2206**	**4**	**0**	**1**	**0.1416**
	MaF9	**4**	**0**	**1**	**0.0500**	**5**	**0**	**0**	**0.0071**	**5**	**0**	**0**	**0.0071**
	MaF10	**5**	**0**	**0**	**0.0373**	**5**	**0**	**0**	**0.0143**	**5**	**0**	**0**	**0.0048**
	MaF11	1	1	3	0.4624	1	1	3	0.4624	1	1	3	0.4624
	MaF12	**5**	**0**	**0**	**0.0071**	**5**	**0**	**0**	**0.0662**	**5**	**0**	**0**	**0.0048**
	MaF13	**4**	**1**	**0**	**0.0864**	**5**	**0**	**0**	**0.0071**	**3**	**1**	**1**	**0.3272**
No. (m)	m=5	**18**	**1**	**2**	**0.0001**	**18**	**1**	**2**	**0.0000**	**17**	**2**	**2**	**0.0162**
	m=8	**20**	**1**	**0**	**0.0284**	**19**	**2**	**0**	**0.0000**	**18**	**1**	**2**	**0.0005**
	m=10	**19**	**1**	**1**	**0.0000**	**18**	**1**	**2**	**0.0001**	**18**	**0**	**3**	**0.0162**
	m=13	**19**	**0**	**2**	**0.0000**	**20**	**0**	**1**	**0.0000**	**18**	**0**	**3**	**0.0477**
	m=15	**20**	**0**	**1**	**0.0000**	**20**	**0**	**1**	**0.0011**	**19**	**0**	**2**	**0.0019**
	All	**96**	**3**	**6**	**0.0000**	**95**	**4**	**8**	**0.0000**	**90**	**3**	**12**	**0.0000**

Furthermore, as observed from the comparisons in the last row of Table II, IRAS+AUM is superior to DRA+AUM, GRA+AUM and IRA+AUM in 96, 95 and 90 out of 105 cases, respectively, and it is inferior to DRA+AUM, GRA+AUM and IRA+AUM in 6, 8 and 12 out of 105 cases, respectively. Furthermore, all the p-values for all the comparisons are close to zero. Hence, it is reasonable to conclude that the proposed IRAS is more efficient for solving MaOPs with different numbers of objectives than the traditional RASs mentioned above.

To have an intuitive observation of the assignment process of the computational resources, Figs. A.2-A.5 of the supplementary file provide the dynamic change of resources in the proposed IRAS during the whole evolutionary process, where the ordinate indicates the number of cloning resources for each individual, the abscissa represents twenty different solutions and *Gen* means the current generation. As we can learn from these figures, different computational resources are allocated for different solutions adaptively at different generations.

D. Comparison with Six Competitive MaOEAs

In this section, six competitors with promising performance, including RVEAiGNG [72], PeEA [73], MOEA/AD [74], MaOEA/IGD [21], MaPSO [75] and hpaEA [26], are adopted for performance comparisons. It should be pointed out that the proposed MaOEA/IRAS was implemented under the jMetal framework [78]. MOEA/AD and MaPSO were also

TABLE III
COMPARISON OF RESULTS OF MaOEA/IRAS AND SIX COMPETITIVE MAOEAS ON WFG41-WFG48 USING HV

Problem	m	RVEAiGNG	PeEA	MOEA/AD	MaOEA/IGD	MaPSO	hpaEA	MaOEA/IRAS
WFG41	5	7.62e-01(1.85e-02)-	7.49e-01(4.90e-03)-	8.01e-01(2.88e-03)-	0.00e+00(0.00e+00)-	6.49e-01(1.48e-02)-	0.00e+00(0.00e+00)-	**8.02e-01(5.12e-03)**
	8	8.61e-01(1.41e-02)-	8.60e-01(8.06e-03)-	8.23e-01(1.87e-02)-	1.07e-01(1.09e-06)-	7.23e-01(1.01e-02)-	6.85e-01(5.69e-02)-	**9.24e-01(2.57e-02)**
	10	9.20e-01(9.10e-03)-	9.06e-01(7.03e-03)-	9.27e-01(3.20e-03)-	1.32e-01(8.23e-02)-	7.44e-01(1.57e-02)-	7.21e-01(3.68e-02)-	**9.39e-01(1.42e-02)**
	13	9.04e-01(1.62e-02)+	**9.07e-01(2.07e-02)+**	7.70e-01(1.20e-02)-	1.71e-01(1.08e-03)-	7.39e-01(2.01e-02)-	6.31e-01(2.99e-02)-	8.73e-01(1.56e-02)
	15	9.21e-01(1.18e-02)-	**9.41e-01(1.63e-02)+**	7.64e-01(4.51e-02)-	1.46e-01(8.23e-02)-	7.79e-01(1.16e-02)-	6.24e-01(5.70e-02)-	9.21e-01(1.88e-02)
WFG42	5	9.80e-01(7.79e-03)-	9.75e-01(4.21e-03)-	9.94e-01(1.50e-03)+	0.00e+00(0.00e+00)-	8.89e-01(7.82e-03)-	0.00e+00(0.00e+00)-	**9.86e-01(3.25e-03)**
	8	9.88e-01(1.50e-03)~	9.90e-01(2.26e-03)-	**9.98e-01(8.76e-04)+**	9.91e-01(4.84e-03)~	8.96e-01(3.85e-03)-	9.85e-01(2.29e-03)~	9.93e-01(3.53e-03)
	10	9.84e-01(2.43e-03)~	9.95e-01(1.36e-03)-	**9.97e-01(8.58e-04)+**	9.92e-01(3.79e-03)~	9.05e-01(1.15e-02)-	9.92e-01(2.04e-03)-	9.96e-01(2.80e-03)
	13	9.88e-01(5.53e-03)-	9.93e-01(1.27e-03)~	9.81e-01(5.18e-03)-	9.71e-01(1.25e-02)-	9.01e-01(1.58e-02)-	9.85e-01(3.08e-03)-	**9.92e-01(3.17e-03)**
	15	9.90e-01(5.47e-03)-	6.03e-01(1.48e-01)-	9.36e-01(1.45e-02)-	9.76e-01(1.11e-02)-	8.90e-01(1.07e-02)-	9.93e-01(1.44e-03)-	**9.96e-01(3.22e-03)**
WFG43	5	2.89e-01(2.55e-02)-	4.84e-01(1.24e-02)-	5.36e-01(7.18e-03)+	0.00e+00(0.00e+00)-	3.16e-01(1.95e-02)-	0.00e+00(0.00e+00)-	**4.94e-01(2.03e-02)**
	8	1.38e-01(3.65e-02)-	**6.35e-01(7.96e-03)+**	4.38e-01(1.61e-02)-	1.15e-01(8.01e-02)-	3.86e-01(4.93e-02)-	3.63e-01(4.44e-02)-	5.19e-01(1.72e-02)
	10	1.21e-01(3.94e-02)-	**6.83e-01(1.63e-02)+**	4.55e-01(3.32e-02)~	9.90e-02(5.00e-05)-	4.85e-01(3.74e-02)~	3.74e-01(2.50e-02)-	5.45e-01(2.72e-02)
	13	**7.30e-01(8.19e-03)+**	6.80e-01(3.64e-02)+	4.38e-01(2.15e-02)~	1.15e-01(1.33e-04)-	4.13e-01(3.88e-02)~	2.91e-01(2.75e-02)-	4.92e-01(6.20e-02)
	15	7.10e-01(3.41e-02)+	**7.77e-01(2.67e-02)+**	3.42e-01(2.63e-02)-	1.24e-01(8.24e-02)-	4.70e-01(5.43e-02)~	3.11e-01(2.92e-02)-	5.51e-01(2.85e-02)
WFG44	5	9.68e-01(1.15e-02)-	9.95e-01(1.28e-03)~	9.94e-01(1.01e-03)~	0.00e+00(0.00e+00)-	9.11e-01(1.63e-02)-	0.00e+00(0.00e+00)-	**9.95e-01(2.10e-03)**
	8	9.91e-01(2.38e-03)~	9.97e-01(8.85e-04)-	**1.00e+00(9.54e-05)+**	9.96e-01(3.11e-03)~	9.23e-01(1.04e-02)-	9.93e-01(7.73e-04)-	9.98e-01(5.03e-04)
	10	9.91e-01(5.41e-03)-	9.97e-01(1.46e-03)~	**1.00e+00(9.91e-05)+**	9.90e-01(8.45e-03)-	9.40e-01(5.78e-03)-	9.97e-01(6.88e-04)-	9.99e-01(6.90e-04)
	13	9.90e-01(4.11e-03)-	9.96e-01(1.34e-03)-	9.98e-01(2.04e-02)~	9.86e-01(5.29e-03)-	9.19e-01(9.73e-03)-	9.95e-01(1.07e-03)~	**9.98e-01(1.45e-03)**
	15	9.98e-01(4.58e-04)-	7.96e-01(1.38e-01)-	9.91e-01(4.59e-03)~	9.88e-01(1.46e-02)-	9.33e-01(6.25e-03)-	9.96e-01(1.55e-03)~	**9.99e-01(4.56e-04)**
WFG45	5	8.41e-01(2.08e-03)-	8.27e-01(3.64e-03)-	8.50e-01(1.34e-03)-	9.89e-02(1.93e-04)-	7.03e-01(1.31e-02)-	8.00e-01(3.23e-02)-	**8.57e-01(1.82e-03)**
	8	9.03e-01(7.68e-03)-	9.16e-01(6.12e-03)-	8.58e-01(1.74e-02)-	1.15e-01(8.01e-02)-	7.32e-01(9.01e-03)-	7.57e-01(2.33e-02)-	**9.46e-01(4.62e-03)**
	10	9.31e-01(8.14e-03)~	9.41e-01(3.46e-03)-	9.45e-01(3.68e-03)-	1.32e-01(8.25e-02)-	7.42e-01(1.25e-02)-	7.57e-01(3.27e-02)-	**9.49e-01(9.21e-03)**
	13	9.10e-01(8.25e-03)+	**9.49e-01(7.10e-03)+**	8.28e-01(1.10e-02)-	1.54e-01(8.13e-02)-	7.13e-01(1.33e-02)-	6.45e-01(3.25e-02)-	9.07e-01(2.59e-02)
	15	9.30e-01(1.27e-02)-	**9.65e-01(9.75e-03)+**	7.36e-01(6.29e-02)-	2.08e-01(7.49e-02)-	7.14e-01(1.90e-02)-	7.20e-01(4.77e-02)-	9.44e-01(1.37e-02)
WFG46	5	9.51e-01(7.00e-03)+	**9.67e-01(1.06e-03)+**	9.65e-01(2.15e-03)+	4.85e-01(1.46e-01)-	8.23e-01(4.39e-03)-	9.51e-01(7.74e-03)+	9.44e-01(1.02e-02)
	8	9.73e-01(8.76e-03)+	**9.88e-01(5.37e-03)+**	9.79e-01(2.78e-03)+	3.43e-01(3.20e-01)-	8.40e-01(7.30e-03)-	9.16e-01(1.99e-02)~	9.50e-01(7.61e-03)
	10	9.71e-01(9.64e-03)+	**9.95e-01(2.52e-03)+**	9.64e-01(5.47e-03)+	3.86e-01(2.63e-01)-	8.15e-01(3.18e-02)-	9.35e-01(1.00e-02)~	9.57e-01(1.12e-02)
	13	9.62e-01(9.55e-03)+	**9.94e-01(2.62e-03)+**	9.15e-01(6.56e-03)-	1.57e-01(8.06e-02)-	8.00e-01(1.48e-02)-	8.71e-01(1.57e-02)~	9.22e-01(1.45e-02)
	15	9.71e-01(8.31e-03)+	**9.99e-01(3.01e-04)+**	8.13e-01(3.54e-02)-	1.57e-01(1.56e-01)-	7.98e-01(3.01e-02)-	9.07e-01(1.61e-02)-	9.55e-01(1.07e-02)
WFG47	5	8.22e-01(1.31e-02)-	8.35e-01(1.97e-03)-	8.54e-01(4.40e-03)-	4.40e-01(1.23e-01)-	7.15e-01(5.16e-03)-	7.91e-01(1.40e-02)-	**8.58e-01(3.78e-03)**
	8	9.11e-01(1.33e-02)~	9.20e-01(3.61e-03)-	8.70e-01(1.49e-02)-	4.62e-01(1.56e-01)-	7.61e-01(1.73e-02)-	7.59e-01(4.57e-02)-	**9.46e-01(1.63e-02)**
	10	9.38e-01(1.52e-03)-	9.43e-01(3.97e-03)-	9.04e-01(2.82e-02)~	4.11e-01(1.25e-01)-	7.80e-01(2.17e-02)-	7.76e-01(3.74e-02)-	**9.47e-01(8.59e-03)**
	13	**9.50e-01(4.37e-03)+**	9.40e-01(1.15e-02)+	6.94e-01(7.11e-02)-	1.44e-01(8.29e-02)-	7.58e-01(1.78e-02)-	6.78e-01(3.00e-02)-	9.07e-01(2.65e-02)
	15	9.57e-01(3.64e-03)+	**9.71e-01(2.86e-03)+**	6.79e-01(1.42e-02)-	1.78e-01(1.72e-01)-	7.78e-01(3.06e-02)-	7.18e-01(5.05e-02)-	9.42e-01(2.70e-02)
WFG48	5	9.81e-01(3.28e-03)+	9.78e-01(3.17e-03)-	**9.92e-01(1.25e-03)+**	9.00e-01(2.41e-02)-	8.84e-01(4.80e-03)-	9.88e-01(1.62e-03)+	9.79e-01(4.03e-03)
	8	9.87e-01(2.66e-03)-	9.90e-01(2.55e-03)-	**9.97e-01(1.06e-03)+**	9.84e-01(5.06e-03)~	8.71e-01(3.36e-03)-	9.84e-01(3.19e-03)~	9.91e-01(5.35e-03)
	10	9.90e-01(4.32e-03)-	9.90e-01(1.94e-03)-	**9.97e-01(5.82e-04)+**	9.85e-01(7.13e-03)~	9.00e-01(1.25e-02)-	9.92e-01(1.34e-03)-	9.92e-01(1.43e-02)
	13	**9.89e-01(5.66e-03)+**	9.75e-01(9.96e-03)-	9.79e-01(5.28e-03)-	9.77e-01(4.36e-03)~	9.01e-01(1.02e-02)-	9.86e-01(4.50e-03)+	9.85e-01(2.03e-02)
	15	9.90e-01(1.70e-03)-	9.06e-01(5.14e-02)-	9.56e-01(8.38e-03)-	9.76e-01(6.91e-03)-	8.80e-01(5.61e-03)-	9.87e-01(5.21e-03)-	**9.91e-01(4.20e-03)**
Best/*All*		3/40	13/40	7/40	0/40	0/40	0/40	**17**/40
–/~/+		22-/5~/13+	22-/3~/15+	23-/6~/11+	34-/6~/0+	37-/3~/0+	30-/7~/3+	– –

implemented under the JMetal framework, while others were implemented in the PlatEMO framework [79].

1) Comparison Results on WFG41-WFG48

Table III provides comparison results in terms of HV for WFG41-WFG48 with 5 to 15 objectives. Some conclusions can be drawn from the HV results listed in Table III. As summarized in the second-to-last row of Table III, MaOEA/IRAS yielded the best results in 17 out of 40 cases, and these compared algorithms, i.e., RVEAiGNG, PeEA, MOEA/AD, MaOEA/IGD, MaPSO and hpaEA, obtained the best results in 3, 13, 7, 0, 0 and 0 out of 40 cases, respectively. From the one-by-one comparisons in the last row of Table III, MaOEA/IRAS performed better than RVEAiGNG, PeEA, MOEA/AD, MaOEA/IGD, MaPSO and hpaEA in 22, 22, 23, 34, 37 and 30 out of 40 cases, respectively, while it was outperformed by them in 13, 15, 11, 0, 0 and 3 out of 40 cases, respectively.

To visually show their comparisons, some final solution sets with the 15th best HV values from all 30 runs are plotted in Figs. A.6-A.10 of the supplementary file, which show the solution's distributions for different problems with various objectives in a high-dimensional objective space. Some conclusions can be easily drawn from these figures. Regarding different test problems with various objectives, all the final solution sets obtained by the proposed MaOEA/IRAS are distributed evenly in these representative problems with different kinds of PFs. The final solution sets obtained by other methods yield relatively poor distributions. Hence, the effectiveness of MaOEA/IRAS in solving WFG4X test problems with different numbers of objectives is further validated.

2) Comparison Results on MaF1-MaF13

Due to page limitations, Table A. XI of the supplementary file summarizes a comparison of the results of all the algorithms considered in terms of the HV for MaF1-MaF13 with 5, 8, 10, 13, and 15 objectives. The results summarized in the second-to-last row of Table A. XI indicate that MaOEA/IRAS displayed superior performance when compared with the other methods, and it yielded the best results in 26 out of 65 cases; the other six compared algorithms obtained the best results in 15, 6, 4, 1, 4 and 9 out of 65 cases. From the one-by-one comparisons in the last row of Table A. XI, MaOEA/IRAS performed better than RVEAiGNG, PeEA, MOEA/AD, MaOEA/IGD, MaPSO and hpaEA in 37, 39, 32, 54, 41 and 38 out of 65 cases, respectively, while being outperformed by these algorithms in 26, 19, 21, 5, 15 and 21 out of 65 cases.

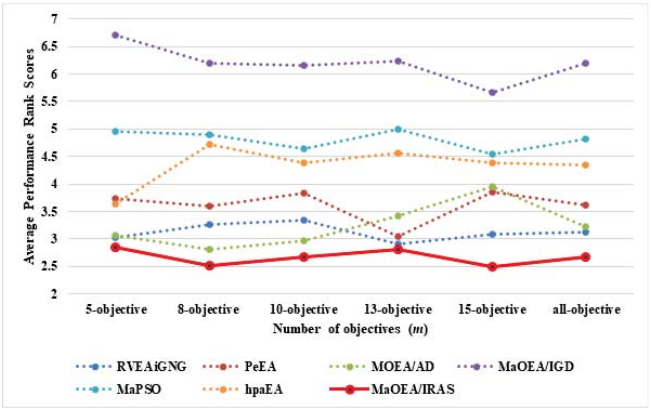

Fig. 5: Average performance rank over all test problems with different numbers of objectives

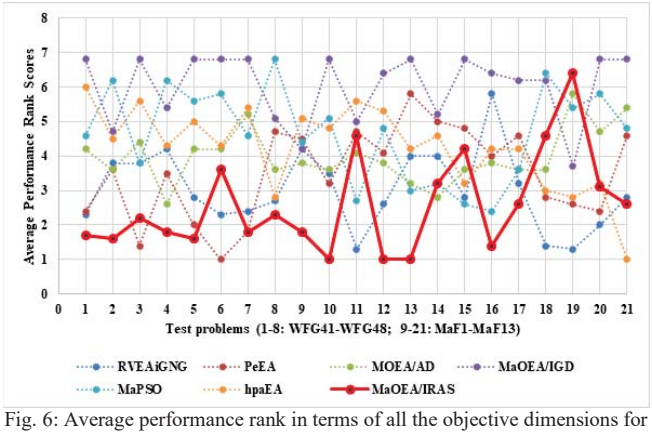

Fig. 6: Average performance rank in terms of all the objective dimensions for all test problems

To visually show their comparisons, some final solution sets with the 15th best HV values from all 30 runs are plotted in Figs. A.11-A.15 of the supplementary file. We can see in these figures that the proposed MaOEA/IRAS can obtain the final solution sets with better distributions than those obtained by the other methods. In other words, the proposed MaOEA/IRAS exhibits effective performance in solving the MaF test problems with various objectives. Hence, the superiority of MaOEA/IRAS over the other methods is further validated in solving the MaF problems.

3) Further Discussion and Analysis of the Overall Performance of the Compared Algorithms.

Furthermore, to verify how well each compared algorithm performs overall, the Friedman's test using the software KEEL was applied to rank all the compared algorithms in all cases.

Fig. 5 summarizes the average performance rank for different numbers of objectives. It should be noted that the ranks of the proposed MaOEA/IRAS are connected by a red line. The last column in Fig. 5 provides the average performance ranks in all the test cases. The average performance rank score of MaOEA/IRAS in all the test problems with all objectives is 2.6714, followed by those of RVEAiGNG (3.1333), MOEA/AD (3.219), PeEA (3.6238), hpaEA (4.3475), MaPSO (4.8095) and MaOEA/IGD (6.1952). Hence, MaOEA/IRAS shows superiority over other methods, as its average performance rank score is smaller for all the test problems.

Fig. 6 provides the average performance rank scores for different problems (WFG41-WFG48 and MaF1-MaF13), and the ranks of MaOEA/IRAS are connected by a red line to easily observe the values. Some conclusions can be drawn from Fig. 6. When considering the WFG4X test problems, MaOEA/IRAS shows an obvious advantage over other methods in most cases except for WFG46, as the average performance rank score of MaOEA/IRAS is larger than those of PeEA and RVEAiGNG. When considering the MaF test problems, our MaOEA/IRAS can obtain the best ranks for most adopted cases. Moreover, MaOEA/IRAS shows competitive performance on solving all MaF problems except for MaF3 with a convex PF, MaF7 with a disconnected PF, and MaF11 with a scaled disconnected PF. Particularly, RVEAiGNG shows the best performance for MaF3 and MaF11, and MaPSO obtains the best result for MaF7. The inferior performance of MaOEA/IRAS on tackling these three problems are mainly because the PFs of these problems are easy to cover and approximate. In the case of sufficient computational resources, our proposed IRAS may not have obvious superiority in solving such problems, as other competitors without RAS can also obtain good results.

In summary, the superiority of MaOEA/IRAS over its competitors when solving most of the test problems adopted in the experiments is verified according to the average performance ranks shown in Fig. 5 and Fig. 6. Furthermore, Table A. XII of the supplementary file provides the comparison results of all the compared algorithms on solving 5-objective MaF and WFG4X test problems based on the IGD values [80], which further validates the favorable performance of MaOEA/IRAS.

E. The Effectiveness of IRAS in Solving the Car-Side-Impact Problem

The performance of the proposed MaOEA/IRAS on solving a real-world engineering optimization problem is further studied in this section. The *Car-Side-Impact* [81] problem with three conflicting objectives and ten constraints is adopted here. As introduced in [81], the main purpose for optimizing this problem is to minimize the weight of a car, the general force experienced by a passenger and the average velocity at which the vehicle strikes a pillar. More details about the *Car-Side-Impact* problem can be read in [81].

It should be noted that the true *PF* is unknown in advance. Thus, the reference *PF* is obtained from all the compared algorithms. First, all the compared algorithms are run to optimize the *Car-Side-Impact* problem 30 times over 1000 generations. Then, 300 nondominated solutions obtained by each algorithm are selected to construct the reference *PF,* which is displayed in Fig. A.16 of the supplementary file.

In our experimental comparisons, the population size N and the maximum number of generations G_{max} are set as 120 and 600, respectively, for the *Car-Side-Impact* problem. Fig. A.17 of the supplementary file plots the final solution set of each compared algorithm. Our proposed IRAS displays advantages in maintaining the population's diversity when compared to traditional RASs (i.e., DRA, GRA and IRA), because the final solutions obtained by IRAS can cover the reference *PF* more evenly and closely than those of other methods. In contrast, the competitors that use traditional RASs have some problems in maintaining diversity as most of their solutions are gathered at the boundary rather than distributed uniformly. Hence, the

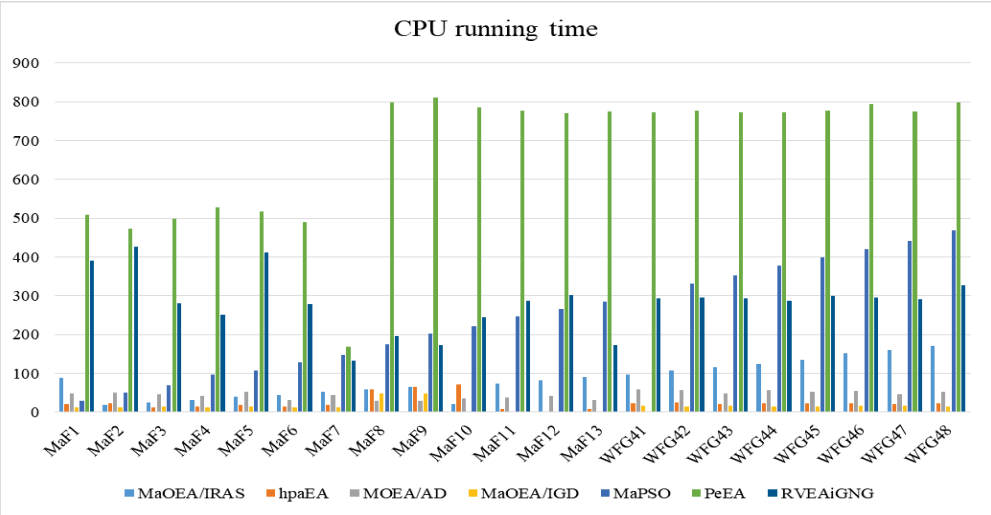

Fig. 7: The average running times (*s*) of all the compared algorithms on MaF1-MaF13 and WFG41-WFG48 with 5 objectives

superiority of IRAS over traditional RASs in solving the *Car-Side-Impact* problem further validates the ability of IRAS on diversity maintenance when solving MaOPs.

F. Computational Complexity Analysis of MaOEA/IRAS

The process of MaOEA/IRAS was given in **Algorithm 1**, which mainly includes three main procedures, i.e., the proposed IRAS process, the evolutionary process and the archive update process. Here, the computational complexities for these three main components of MaOEA/IRAS are analyzed as follows. First, the population P with N solutions is used to perform the IRAS process, which requires a time complexity of $O(mN^2)$, where m is the number of objectives and N indicates the population size. After that, two evolutionary operators, including SBX and PM, are performed on the cloned population C with N solutions, which needs a time complexity of $O(mN)$. The archive update process is run on the union population with $2N$ solutions, which requires a total time complexity of $O(m|U||K|)$. As introduced above, $|U|$ and $|K|$ are, respectively, equal to $2N$ and $\lceil N\times(m-1)/m\rceil$. Hence, the total complexity for the archive update process is also $O(mN^2)$. Therefore, the overall worst time complexity of the proposed MaOEA/IRAS is $O(mN^2)$ in one generation. Moreover, the space complexity of MaOEA/IRAS is $O(N)$.

In order to evaluate the actual runtime of MaOEA/IRAS, the average running times of all the compared algorithms (in seconds: *s*) from 30 independent runs are plotted in Fig. 7, for MaF1-MaF13 and WFG41-WFG48 with 5 objectives. Obviously, PeEA showed the lowest speed, because the on-line PF shape estimation method and the adaptive scalarizing function adopted in PeEA are very time-consuming, followed by REVAiGNG and MaPSO. Our proposed MaOEA/IRAS had the similar executing efficiency with MOEA/AD and hpaEA. Finally, MaOEA/IGD showed the fastest speed as it was implemented in a simple framework. Therefore, we can conclude that our proposed MaOEA/IRAS not only can address various MaOPs effectively, but also has acceptable execution times.

V. Conclusions and Future Work

In this paper, an immune-inspired resource allocation strategy (IRAS) is proposed for solving MaOPs; this approach enhances the ability of RASs to maintain diversity in a high-dimensional objective space. According to the principles of the proposed IRAS, the solutions with large diversity distances will have more clones than other solutions, which reflects the assignment of computational resources to sparse regions. Thus, the diversity of the population can be maintained. Moreover, to provide high-quality solutions for the cloning operator, an efficient archive update mechanism (AUM) with two selection rounds is designed, where the distribution of the population is guaranteed in the first round and the convergence pressure is strengthened during the second round. Hence, a good balance between the diversity and the convergence is achieved by using AUM. When compared to three well-known RASs, including DRA, GRA and IRA, and six competitive algorithms, including RVEAiGNG, PeEA, MOEA/AD, MaOEA/IGD, MaPSO and hpaEA, the proposed MaOEA/IRAS showed some advantages, especially in some test problems with irregular and convex PFs. Moreover, when solving the practical *Car-Side-Impact* problem, the proposed IRAS also performed better than other traditional RASs.

Although our proposed IRAS has shown an obvious improvement for solving MaOPs when compared to most traditional RASs, the ability of IRAS for tackling MaOPs with extremely convex/concave PFs needs to be further studied. In addition, the performance of IRAS for solving large-scale MOPs (e.g., MaF14-MaF15 [44]) that involve a large number of decision variables also deserves further study. Hence, in our future work, the proposed IRAS will be further studied to enhance its performance for solving MaOPs with extremely convex/concave PFs or large-scale decision variables. Moreover, MaOEA/IRAS will be also extended to tackle more real-world engineering problems in our future work.

References

[1] Q.Z. Lin, S.B. Liu, K.C. Wong, M.G. Gong, C.A. Coello Coello, J.Y. Chen and J. Zhang, "A Clustering-Based Evolutionary Algorithm for

Many-Objective Optimization Problems," IEEE Trans. Evol. Comput., vol. 23, no. 3, pp. 391–405, June. 2019.
[2] X.Y. He, Y.R. Zhou and Z.F. Chen, "An Evolution Path-Based Reproduction Operator for Many-Objective Optimization," IEEE Trans. Evol. Comput., vol. 23, no. 1, pp. 29–43, February. 2019.
[3] M. Elarbi, S. Bechikh, A. Gupta, L. Ben Said and Y. Ong, "A New Decomposition-Based NSGA-II for Many-Objective Optimization," IEEE Trans. Systems, Man, and Cybern.: Syetems. vol. 48, no. 7, pp. 1191-1210, July 2018.
[4] H.P. Ma, M.R. Fei, Z.H. Jiang, L. Li, H.Y. Zhou and D. Crookes, "A Multipopulation-Based Multiobjective Evolutionary Algorithm," IEEE Trans. Cybern., vol. 50, no. 2, pp. 689–702, February. 2020.
[5] K. Miettinen, "Nonlinear Multiobjective Optimization," Boston, Ma, USA: Kluwer Academic, 1999.
[6] X. Wang, Z. Dong and L. Tang, "Multiobjective Differential Evolution With Personal Archive and Biased Self-Adaptive Mutation Selection," IEEE Trans. Systems, Man, and Cybern.: Syetems. Vol. 50, no. 12, pp. 5338-5350, December 2020.
[7] J.H. Wang, G.X Liang and J. Zhang, "Cooperative Differential Evolution Framework for Constrained Multiobjective Optimization," IEEE Trans. Cybern., vol. 49, no. 6, pp. 2060–2072, June. 2019.
[8] G. Yu, Y.C. Jin and M. Olhofer, "A Multiobjective Evolutionary Algorithm for Finding Knee Regions Using Two Localized Dominance Relationship," IEEE Trans. Evol. Comput., vol. 25, no. 1, pp. 145–158, Feb. 2021.
[9] Y.R. Naidu and A.K. Ojha, "Solving Multiobjective Optimization Problems Using Hybrid Cooperative Invasive Weed Optimization With Multiple Populations," IEEE Trans. Systems, Man, and Cybern.: Syetems. vol. 48, no. 6, pp. 821-832, June 2018.
[10] C.J. Zhang, L. Gao, X.Y. Li, W.M. Shen, J.J. Zhou, and K.C. Tan, "Resetting Weight Vectors in MOEA/D for Multiobjective Optimization Problems With Discontinuous Pareto Front," IEEE Trans. Cybern. vol. 52, no. 9, pp. 9770–9783, September. 2022.
[11] H.K. Chen, G.H. Wu, W. Pedrycz, P.N. Suganthan, L.N. Xing, and X.M Zhu, "An Adaptive Resource Allocation Strategy for Objective Space Partition-Based Multiobjective Optimization," IEEE Trans. Systems, Man, and Cybern.: Syetems. vol. 51, no. 3, pp. 1507–1522, March. 2021.
[12] Y. Tian, C. He, R. Cheng and X. Zhang, "A Multistage Evolutionary Algorithm for Better Diversity Preservation in Multiobjective Optimization," IEEE Trans. Systems, Man, and Cybern.: Syetems. vol. 51, no. 9, pp. 5880–5894, September. 2021.
[13] J.H. Wang, Y.Y. Li, Q.F. Zhang, Z.Z. Zhang and S.C. Gao, "Cooperative Multiobjective Evolutionary Algorithm With Propulsive Population for Constrained Multiobjective Problems," IEEE Trans. Systems, Man, and Cybern.: Syetems. vol. 52, no. 6, pp. 3476–3491, June. 2022.
[14] X.Y. Cai, Y.S. Xiao, M.Q. Li, H. Hu, H. Ishibuchi and X.P. Li, "A Grid-Based Inverted Generational Distance for Multi/Many-Objective Optimization," IEEE Trans. Evol. Comput., vol. 25, no. 1, pp. 21–34, February. 2021.
[15] Z.Z Liu, Y. Wang, B.C. Wang, "Indicator-based Constrained Multiobjective Evolutionary Algorithms," IEEE Trans. Systems, Man, and Cybern.: Syetems. vol. 51, no. 9, pp. 5414–5426, September. 2021.
[16] N. Beume, B. Naujoks, and M. Emmerich, "SMS-EMOA: Multiobjective selection based on dominated hypervolume," European Journal of Operational Research, vol. 181, no. 3, pp. 1653–1669, 2007.
[17] G. Yu, Y.C. Jin and M. Olhofer "Benchmark Problems and Performance Indicators for Search of Knee Points in Multiobjective Optimization," IEEE Trans. Cybern., vol. 50, no. 8, pp. 3531–3544, Aug. 2020.
[18] Y. Tian, R. Cheng, X. Zhang, F. Cheng, and Y. Jin, "An Indicator-Based Multiobjective Evolutionary Algorithm with Reference Point Adaptation for Better Versatility," IEEE Trans. Evol. Comput., vol. 22, no. 4, pp. 609–622, August. 2018.
[19] H. Ishibuchi, N. Akedo, and Y. Nojima, "Behavior of Multiobjective Evolutionary Algorithms on Many-objective Knapsack Problems," IEEE Trans. Evol. Comput., vol. 19, no. 2, pp. 264–283, April. 2015.
[20] B. Li, J. Li, K, Tang, and X. Yao, "Many-objective Evolutionary Algorithms: A survey," ACM Comput. Surveys, vol.48, no.1, pp. 45-76, March, 2011.
[21] H.K. Chen, Y. Tian, W. Pedrycz, G.H. Wu, R. Wang and L. Wang, "Hyperplane Assisted Evolutionary Algorithm for Many-Objective Optimization Problems," IEEE Trans. Cybern., vol. 50, no. 7, pp. 3367–3380, July. 2020.
[22] W.B. Qiu, J.H. Zhu, G.H. Wu, M.F. Fan and P.N. Suganthan, "Evolutionary Many-objective Algorithm based on Fractional Dominance Relation and Improved Objective Space Decomposition Strategy," Swarm and Evol. Comput., vol. 60, 100776, 2021.
[23] X.Y. He, Y.R. Zhou, Z.F. Chen and Q.F. Zhang, "Evolutionary Many-Objective Optimization Based on Dynamical Decomposition," IEEE Trans. Evol. Comput., vol. 23, no. 3, pp. 361–375, June. 2019.
[24] S.B. Liu, Q.Z. Lin, K.C. Wong, C.A. Coello Coello, J.Q. Li, Z. Ming and J. Zhang, "A Self-Guided Reference Vector Strategy for Many-Objective Optimization," IEEE Trans. Cybern., vol. 52, no. 2, pp. 1164–1178, February. 2022.
[25] Y.H. Zhang, Y.J. Gong, T.L. Gu, H.Q. Yuan, W. Zhang, S. Kwong and J. Zhang, "DECAL: Decomposition-Based Coevolutionary Algorithm for Many-Objective Optimization," IEEE Trans. Cybern., vol. 49, no. 1, pp. 27–41, January. 2019.
[26] Y.N. Sun, G.G. Yen and Z. Yi, "IGD Indicator-Based Evolutionary Algorithm for Many-Objective Optimization Problems," IEEE Trans. Evol. Comput., vol. 23, no. 2, pp. 173–187, April. 2019.
[27] T. Pamulapati, R. Mallipeddi and P.N. Suganthan, "ISDE+-An indicator for multi and many-objective optimization," IEEE Trans. Evol. Comput., vol. 23, no. 2, pp. 346–352, April. 2019.
[28] W.B. Qiu, J.H. Zhu, G.H. Wu, H.K. Chen, W. Pedrycz and P.N. Suganthan, "Ensemble Many-objective Optimization Algorithm Based on Voting Mechanism," IEEE Trans. Systems, Man, and Cybern.: Syetems. vol. 52, no. 3, pp. 1716–1730, March. 2022.
[29] Q.F. Zhang, W.D. Liu and H. Li, "The Performance of a New Version of MOEA/D on CEC09 unconstrained MOP instances," *Proceeding of* the IEEE Congress on Evolut. Comput., Trondheim, Norway, pp. 18-21, May, 2009.
[30] A. Zhou and Q. Zhang, "Are All the Subproblems Equally Important? Resource Allocation in Decomposition-based Multiobjective Evolutionary Algorithms," IEEE Trans. Evol. Comput., vol. 20, no. 1, pp. 52–64, February. 2016.
[31] Q.Z. Lin, G.M. Jin, Y.P. Ma, K.C. Wong, C.A. Coello Coello, J.Q. Li, J.Y. Chen and J. Zhang, "A Diversity-Enhanced Resource Allocation Strategy for Decomposition-Based Multiobjective Evolutionary Algorithm," IEEE Trans. Cybern., vol. 48, no. 8, pp. 2388–2401, August. 2018.
[32] Z.K. Wang, Y.O. Ong, J.Y. Sun, A. Gupta and Q.F. Zhang, "A Generator for Multiobjective Test problems with Difficult-to Approximate Pareto Front Boundaries," IEEE Trans. Evol. Comput., vol. 23, no. 4, pp. 556–571, August. 2019.
[33] Q. Kang, X.Y. Song, M.C. Zhou and L. Li, "A Collaborative Resource Allocation Strategy for Decomposition-based Multiobjective Evolutionary Algorithms," IEEE Trans. Systems, Man, and Cybern.: Syetems. vol. 49, no. 12, pp. 2416–2423, December. 2019.
[34] P. Wang *et.al*, "A New Resource Allocation Strategy Based on Relationship between Subproblems for MOEA/D," Inf. Sci., vol. 50, pp. 337-362, 2019.
[35] K. Li, A. Fialho, S. Kwong and Q.F. Zhang, "Adaptive Operator Selection with Bandits for a Multiobjective Evolutionary Algorithm Based on Decomposition," IEEE Trans. Evol. Comput., vol. 18, no. 1, pp. 114–130, February. 2014.
[36] W.J. Wang, S.Q. Yang, Q.Z. Lin, Q.F. Zhang, K.C. Wong, C.A. Coello Coello and J.Y. Chen, "An Effective Ensemble Framework for Multiobjective Optimization," IEEE Trans. Evol. Comput., vol. 23, no. 4, pp. 645–659, August. 2019.
[37] Y.T. Qi, X.L. Ma, F. Liu, L.C. Jiao, J.Y. Sun and J.S Wu, "MOEA/D with Adaptive Weight Adjustment," Evolut. Comput., vol.22, no. 2, pp. 231-264, June, 2014.
[38] P. Wang, B. Liao, W. Zhu, L.J. Cai, S.Q. Ren, M. Chen, Z.J. Li and K.Q. Lin, "Adaptive Region Adjustment to Improve the Balance of Convergence and Diversity in MOEA/D," Appl. Soft Computing, vol.70, pp. 797-813, 2018.
[39] L.P. Wang, W. Yu, F.Y. Qiu, J.F. Lu and P. Fu, "Preference-inspired Coevolutionary Algorithm based on Differentiated Space for Many-objective Problems," Soft Computing, vol. 25, pp. 819-833, 2021.
[40] H.K. Chen, G.H. Wu, W. Pedrycz, P.N. Suganthan, L.N. Xing and X.M. Zhou, "An Adaptive Resources Allocation Strategy for Objective Space Partition-based Multiobjective Optimization," IEEE Transactions on Systems, Man, and Cybernetics: Systems, vol. 51, no. 3, pp. 1507-1522, March 2021.
[41] A. Trivedi, D. Srinivasan, K. Sanyal, and A. Ghosh, "A Survey of Multiobjective Algorithms based on Decomposition," IEEE Trans. Evol. Comput., vol. 21, no. 3, pp. 440–462, June. 2017.
[42] Y.R. Zhou, Y. Xiang, Z.F. Chen, J. He, and J.H. Wang, "A Scalar Projection and Angle-based Evolutionary Algorithm for Many-objective Optimization Problems," IEEE Trans. Cybern., vol. 49, no. 6, pp. 2073–2084, June. 2019.
[43] R. Wang, R.C. Purshouse, P.J. Fleming, "Preference-inspired Co-evolutionary Algorithms Using Weight Vectors," Rur. J. Oper. Res., vol. 243, no. 2, pp. 423-441, June. 2015.
[44] R. Cheng, M.Q. Li, Y. Tian, X.Y. Zhang, S.X. Yang, Y.C. Jin and X. Yao, "A Benchmark Test Suite for Evolutionary Many-objective Optimization," Complex & Intell. Syst., vol. 3, no.1, pp. 67-81, February 2017.
[45] Q. F. Zhang and H. Li, "MOEA/D: A Multiobjective Evolutionary Algorithm based on Decomposition," IEEE Trans. Evol. Comput., vol. 11, no. 6, pp. 712–731, December. 2007.
[46] H.L. Liu, K. Miettinen, and K. Deb, "Dcomposition of a Multiobejctive Optimization Problem into a Number of Single Multiobjective Subproblems," IEEE Trans. Evol. Comput., vol. 18, no. 3, pp. 450–455, June. 2014.
[47] H.L. Liu, L. Chen, Q.F. Zhang, and K. Deb, "Adaptively Allocating Search Effort in Challenging Many-objective Optimization Problems," IEEE Trans. Evol. Comput., vol. 22, no. 3, pp. 433–448, June. 2018.
[48] H. Ishibuchi, Y. Setoguchi, H. Masuda, and Y. Nojima, "Performance of Decomposition-based Many-objective Algorithms Strongly Depends on

ParetoFront Shapes," IEEE Trans. Evol. Comput., vol. 21, no. 2, pp. 169–190, April. 2017.
[49] H. Ishibuchi, R. Imada, Y. Setoguchi, and Y. Nojima, "Reference Point Specification in Inverted Generational Distance for Triangular Linear Pareto Front," IEEE Trans. Evol. Comput., vol. 22, no. 6, pp. 961–975, December. 2018.
[50] Z.N. He, G.G. Yen, "Many-objective Evolutionary Algorithm based on Coordinated Selection Strategy," IEEE Trans. Evol. Comput., vol. 21, no. 2, pp. 220–233, Apr. 2017.
[51] Q. Liu, Y. Jin, M. Heiderich and T. Rodemann, "Coordinated Adaptation of Reference Vectors and Scalarizing Functions in Evolutionary Many-objective Optimization," IEEE Transactions on Systems, Man, and Cybernetics: Systems, 2022, doi: 10.1109/TSMC.2022.3187370.
[52] S.B. Liu, Q.Z. Lin, K.C. Tan, M.G. Gong, and C.A. Coello Coello, "A Fuzzy Decomposition-Based Multi/Mant-Objective Evolutionary Algorithm," IEEE Trans. Cybern., vol. 52, no. 5, pp. 3495–3509, May. 2022.
[53] M. Li and X. Yao, "What Weights Work for You? Adapting Weights for Any Pareto front Shape in Decomposition-based Evolutionary Multi-objective Optimization," Evol. Comput., vol. 28, no. 2, pp. 227–253, 2020.
[54] Y. Tian, R. Cheng, X. Zhang, and Y. Jin, "An Indicator based Multi-objective Evolutionary Algorithm with Reference Point Adaptation for Better Versatility," IEEE Trans. Evol. Comput., vol. 22, no. 4, pp. 609–622, Aug. 2018.
[55] Y. Yuan, H. Xu, B. Wang and X. Yao, "Balancing Convergence and Diversity in Decomposition-Based Many-Objective Optimizers," IEEE Trans. Evol. Comput., vol. 20, no. 2, pp. 180–198, April. 2016.
[56] K. Shang, H. Ishibuchi, L.J. He and L.M. Pang, "A Survey on the Hypervolume Indicator in Evolutionary Multiobjective Optimization," IEEE Trans. Evol. Comput., vol. 25, no. 1, pp. 1–20, Feb. 2021.
[57] K. Deb and R. B. Agrawal, "Simulated Binary Crossover for Continuous Search Space," Complex Systems, vol. 9, no. 3, pp. 115–148, 1994.
[58] H. Li, Q.F. Zhang, "Multi-objective Optimization Problems with Complicated Pareto sets, MOEA/D and NSGA-II," IEEE Trans. Evol. Comput., vol. 13, no. 2, pp. 284–302, April. 2009.
[59] W.W. Zhang, G.G. Yen, and Z.S. He, "Constrained Optimization via Artificial Immune Systems," IEEE Trans. Cybern., vol. 44, no. 2, pp. 185–198, February. 2014.
[60] K.M. Woldemariam, and G.G. Yen, "Vaccine-enhanced Artificial Immune System for Multimodal Function Optimization," IEEE Trans. Systems, Man, and Cybern. Part B: Cybern., vol. 40, no. 1, pp. 218-228, February, 2010.
[61] L.J. Li, Q.Z. Lin, and Z. Ming, "A Survey of Artificial Immune Algorithm for Multi-objective Optimization," Neurocomputing, vol. 489, pp. 211-229, June, 2022.
[62] L.J. Li, Q.Z. Lin, K. Li and Z. Ming, "Vertical Distance-based Clonal Selection Mechanism for the Multiobjective Immune Algorithm," Swarm and Evol. Comput., vol. 63, June. 2021: 100886.
[63] M.G. Gong, L.C. Jiao, H.F. Du, and L.F. Bo, "Multiobjective Immune Algorithm with Nondominated Neighbor-based Selection," Evol. Comput., vol. 16, no. 2, pp. 225–255, November. 2009.
[64] J.S. Chun, H.K. Jung, and S.Y. Hahn, "A Study on Comparison of Optimization Performances between Immune Algorithm and Other Heuristic Algorithms," IEEE Trans. Magn., vol. 34, no. 5, pp. 2972-2975, September, 1998.
[65] M. Elarbi, S. Bechikh, A. Gupta, L. Ben Said and Y. Ong, "A New Decomposition-Based NSGA-II for Many-Objective Optimization," IEEE Trans. Systems, Man, and Cybern.: Syetems. vol. 48, no. 7, pp. 1191-1210, July 2018.
[66] B. Wang, H. Li, Q. Zhang and Y. Wang, "Decomposition-Based Multiobjective Optimization for Constrained Evolutionary Optimization," IEEE Trans. Systems, Man, and Cybern.: Syetems. Vol 51, no.1, pp. 574-587, 2021.
[67] S.B. Liu, Q.Y. Yu, Q.Z. Lin and K.C. Tan, "An Adaptive Clustering-based Evolutionary Algorithm for Many-objective Optimization Problems," Inform. Sci., vol.537, pp. 261-283, October, 2020.
[68] S.Y. Jiang and S.X. Yang, "A Strength Pareto Evolutionary Algorithm Based on Reference Direction for Multiobjective and Many-objective Optimization," IEEE Trans. Evol. Comput., vol. 21, no. 3, pp. 329–346, June. 2017.
[69] Y.C. Hua, Y.C. Jin, and K.R. Hao, "A Clustering-based Adaptive Evolutionary Algorithm for Multiobjective Optimization With Irregular Pareto Fronts," IEEE Trans. Cybern., vol. 49, no. 7, pp. 2758–2770, July. 2019.
[70] H. Ishibuchi, Y. Hitotsuyanagi, N. Tsukamoto, and Y. Nojima, "Manyobjective Test Problems to Visually Examine the Behavior of Multiobjective Evolution in a Decision Space," in *Proc*. Int. Conf. Parallel. Prob. Solving Nat., Krakow, Poland, 2010, pp. 91-100.
[71] L. White, L. Bradstreet, and L. Barone, "A Fast Way of Calculating Exact Hypervolumes," IEEE Trans. Evol. Comput., vol. 16, no. 1, pp. 86–95, Feb. 2012.
[72] Q.Q. Lin, Y.C. Jin, M. Heiderich, T. Rodemann, and G. Yu, "An Adaptive Reference Vector-guided Evolutionary Algorithm Using Growing Neural Gas for Many-objective optimization of Irregular Problems", IEEE Trans. Cybern., vol. 52, no. 5, pp. 2698–2711, May. 2022.
[73] L. Li, G.G. Yen, A. Sahoo, L. Chang, and T.L. Gu, "On the Estimation of Pareto Front and Dimensional Similarity in Many-objective Evolutionary Algorithm," Information Sciences, vol. 563, pp. 375-400, 2021.
[74] M.Y. Wu, K. Li, S. Kwong, Q.F. Zhang, "Evolutionary Many-Objective Optimization Based on Adversarial Decomposition," IEEE Trans. Cybern., vol. 50, no. 2, pp. 753–764, February. 2020.
[75] Y. Xiang, Y. Zhou, Z. Chen, and J. Zhang, "A Many-objective Particle Swarm Optimizer with Leaders Selected from Historical Solutions by using Scalar Projections," IEEE Trans. Cybern., vol. 50 no. 5, pp. 2209-2222, May. 2020.
[76] R. Cheng, Y.C. Jin, M. Olhofer and B. Sendhoff, "A Reference Vector Guided Evolutionary Algorithm for Many-Objective Optimization," IEEE Trans. Evol. Comput., vol. 20, no. 5, pp. 773–791, October. 2016.
[77] J. Alcala-Fdez et al., "KEEL: A Software Tool to Assess Evolutionary Algorithms for Data Mining Problems," Soft Comput., vol. 13, no. 3, pp. 307–318, 2009.
[78] J. J. Durillo and A. J. Nebro, "JMETAL: A Java Framework for Multi-objective Optimization," Adv. Eng. Softw., vol. 42, no. 10, pp. 760–771, 2011.
[79] Y. Tian, R. Cheng, X. Zhang, and Y. Jin, "PlatEMO: A MATLAB Platform for Evolutionary Multi-objective Optimization [educational forum]," IEEE Comput. Intell. Mag., vol. 12, no. 4, pp. 73–87, November. 2017.
[80] G. Chen, Y. Guo, M. Huang, D. Gong, and Z. Yu, "A Domain Adaptation Learning Strategy for Dynamic Multiobjective Optimization," Inf. Sci., vol. 606, no. 4, pp. 328–349, Aug. 2022.
[81] H. Jain and K. Deb, "An Evolutionary Many-objective Optimization Algorithm Using Reference-point based Nondominated Sorting Approach, Part II: Handing Constraints and Extending to An AdaptiveApproach," IEEE Trans. Evol. Comput., vol. 18 no. 4, pp. 602–622, August. 2014.

Lingjie Li received the B.S. degree from Shandong Technology and Business University, Yantai, China in 2017, the M.S. degree from Shenzhen University, Shenzhen, China in 2020, and visited University of Exeter, Exeter, UK, as a visiting student in 2019.

He is currently pursuing his Ph.D. degree in College of Computer Science and Software Engineering, Shenzhen University. He focuses on research in the area of Evolutionary Computation, including algorithm researches on multi/many-objective optimization, large-scale optimization, and application researches on feature selection, cloud/edge computing, and remote sensing hyperspectral images.

Qiuzhen Lin (Member IEEE) received the B.S. degree from Zhaoqing University and the M.S. degree from Shenzhen University, China, in 2007 and 2010, respectively. He received the Ph.D. degree from Department of Electronic Engineering, City University of Hong Kong, Kowloon, Hong Kong, in 2014.

He is currently an associate professor in College of Computer Science and Software Engineering, Shenzhen University. He has published over sixty research papers since 2008. His current research interests include artificial immune system, multi-objective optimization, and dynamic system.

Zhong Ming received the Ph.D. degree in Computer Science and Technology from the Sun Yat-Sen University, Guangzhou, China, in 2004.

He is currently the Executive Director of the Graduate School of Shenzhen University, and a Professor with the National Engineering Laboratory for Big Data System Computing Technology and the College of Computer Science and Software Engineering, Shenzhen University, Shenzhen, China. His research interests include software engineering and artificial intelligence. He has published more than 200 refereed international conference and journal papers (including 40+ ACM/IEEE Transactions papers). He was the recipient of the ACM TiiS 2016 Best Paper Award and some other best paper awards.

Ka-Chun Wong received the B.Eng. degree in computer science and the M.Phil. degree from United College, Chinese University of Hong Kong, Hong Kong, in 2008, and 2010, respectively, and the Ph.D. degree from the Department of Computer Science, University of Toronto, Toronto, ON, Canada, in 2014.

He is an Associate Professor with the City University of Hong Kong, Hong Kong,. His research interests include bioinformatics, computational biology, evolutionary computation, data mining, machine learning, and interdisciplinary research.

Dr. Wong is the Associate Editor of BioData Mining and CMES. He is also on the editorial board of Applied Soft Computing, Journal of Biomedical Informatics, and PeerJ Computer Science.

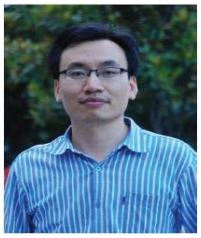

Maoguo Gong (Senior Member, IEEE) received the B.S. and Ph.D. degrees in electronic science and technology from Xidian University, Xi'an, China, in 2003 and 2009, respectively.

Since 2006, he has been a Teacher with Xidian University. In 2008 and 2010, he was promoted as an Associate Professor and a Full Professor, respectively, both with exceptive admission. His current research interests include computational intelligence with applications to optimization, learning, data mining, and image understanding.

Dr. Gong was a recipient of the Prestigious National Program for the support of Top-Notch Young Professionals from the Central Organization Department of China, the Excellent Young Scientist Foundation from the National Natural Science Foundation of China, and the New Century Excellent Talent in University from the Ministry of Education of China. He is the Vice Chair of the IEEE Computational Intelligence Society Task Force on Memetic Computing, an Executive Committee Member of the Chinese Association for Artificial Intelligence, and a Senior Member of the Chinese Computer Federation. He is also an Associate Editor of the IEEE TRANSACTIONS ON EVOLUTIONARY COMPUTATION.

Carlos A. Coello Coello (Fellow, IEEE) received the Ph.D. degree in computer science from Tulane University, New Orleans, LA, USA, in 1996.

He is a Professor (CINVESTAV-3F Researcher) with the Department of Computer Science of CINVESTAV-IPN, Mexico City, Mexico. He has authored and coauthored over 450 technical papers and book chapters. He has also coauthored the book *Evolutionary Algorithms for Solving Multi-Objective Problems* (Second Edition, Springer, 2007). His publications currently report over 57 600 citations in Google Scholar (his H-index is 95). His research interests include evolutionary multiobjective optimization and constraint-handling techniques for evolutionary algorithms.

Dr. Coello Coello was a recipient of the 2007 National Research Award from the Mexican Academy of Sciences in the area of *Exact Sciences*, the 2013 IEEE Kiyo Tomiyasu Award, and the 2012 National Medal of Science and Arts in the area of Physical, Mathematical and Natural Sciences. He is currently the Editor-in-Chief of the IEEE TRANSACTIONS ON EVOLUTIONARY COMPUTATION. He is a member of the Association for Computing Machinery and the Mexican Academy of Science.